



A study of a fractal multi-pantograph delay model with varying coefficients using fractional-order wavelets

Deepak Singh and Sag Ram Verma*

Department of Mathematics and Statistics, Gurukula Kangari (Deemed to be University), Haridwar, 249404, Uttarakhand, India.

Abstract

Apart from using fractal dimensions to describe statistical self-similarity, exploring a direct measurement approach involves considering mathematical models capable of constructing a real-world fractal entity, as classical differential and integral operators cannot efficiently handle such problems. In this study, the fractal derivative is applied to develop a fractal model for multi-pantograph delay differential equations with variable coefficients. The wavelet approach, employing Jacobi fractional order wavelets, has been developed to attain a numerical solution. The proposed methodology relies on the utilization of the fractal integral operational matrix of Jacobi fractional-order wavelets combined with the collocation method. We have outlined pseudo-code and conducted a stability analysis for the methods proposed within the specified model. Furthermore, the convergence analysis of the approximate solution is presented through some lemmas and theorems. The numerical results and error analysis of some illustrative examples are also shown in the tables and graphs. In the proposed methods, numerical results are derived across various values of the fractal (μ) and fractional (ϕ) parameters. It is important to highlight that the classical scenario is retrieved when $\mu = 1$.

Keywords. Fractal operator, Multi-pantograph delay differential equation, Fractional order Jacobi wavelets, Function approximation, Integral operational matrix.

2010 Mathematics Subject Classification. 41A30, 47N20, 34A12.

1. INTRODUCTION

In recent decades, the classical calculus modeling approach has found difficulty in describing an increasing number of complex scientific and engineering problems. In both applied mathematics and pure mathematics, a non-traditional form of derivative, such as fractional, fractal and fractal-fractional derivative are recognized [1, 3, 11, 15, 29]. In the current work, we focus on fractal derivative, in which the variable is scaled according to t^μ , where μ is the fractal dimension [23, 43]. The continuous but non-differentiable functions admit the fractal (local fractional) derivatives, which can be regarded as the generalization of usual derivatives [19, 42]. Fractal derivatives originate from the fractal time-space metric and consequently, can accurately represent the inherent fractal structure of turbulence [9, 10, 44].

Moreover, the fractal structure and fractured systems were initially identified in 1985 during an investigation into nuclear waste disposal sites [6], and numerous authors have subsequently confirmed this relationship [34, 35]. The concept of fractal structure arises from the observation that natural irregular objects often display recurring patterns at various scales, known as self-similarity. This field encounters challenges in measuring fractal dimensions due to various mechanical issues and the need to address numerical and experimental noise along with data constraints. Despite these obstacles, it has attracted attention from researchers and is experiencing rapid growth. The assessment of fractal dimensions for statistically self-similar singularities has practical implications across the various fields, such as electrochemical processes [2], neuroscience, physics, image analysis, diagnostic imaging, physiology, and Riemann zeta zeros [24].

Received: 01 July 2024; Accepted: 22 April 2025.

* Corresponding author. Email: drsverma@gkv.ac.in.

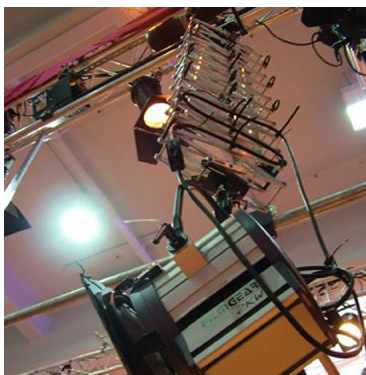


FIGURE 1. A studio pantograph model [38].

In this study, we assumed the generalized form of a multi-pantograph delay differential equation (MPDDEs) with variable coefficients [16, 27, 39] and created its fractal form, such as

$${}^{FO}\mathfrak{D}_t^\mu \xi(t) = f(t, \xi(t), \xi(k_1t), \xi(k_2t), \dots, \xi(k_lt)), \quad t \geq 0, \tag{1.1}$$

with initial condition

$$\xi(0) = \xi_0,$$

where $0 < k_i < 1$; for $i = 1, 2, 3, \dots, l$ and ${}^{FO}\mathfrak{D}_t^\mu$ denotes the fractal derivative of function $\xi^\nu(t)$ with fractal order $\mu \in (0, 1]$, which is defined in subsection 2.1. The Eq.(1.1) is referred to as fractal-MPDDEs (FMPDDEs) and can be reformulated as follows,

$${}^{FO}\mathfrak{D}_t^\mu \xi(t) = p(t) \xi(t) + \sum_{i=1}^l q_i(t) \xi(k_it) + F(t), \quad 0 \leq t < 1, \tag{1.2}$$

with initial condition

$$\xi(0) = \xi_0.$$

This specific class of delay differential equations (DDEs) manifests in numerous real-world scenarios, encompassing electronic systems [45], population dynamics, dynamical systems [26], quantum mechanics, traffic models, biological systems, navigational control of aircraft, and economic contexts, etc. [5, 18, 25]. DDEs constitute a unique class of differential equations that consider both the current state and previous states of a system. Moreover, in the domain of DDEs, there has been relatively more focus on functional differential equations (FDEs), particularly pantograph delay differential equations (PDDEs). The concept of PDDEs originated from the investigations conducted by Ockendon and Tayler [28, 41], where they studied the interaction between the pantograph head of an electric locomotive and the overhead power supply. Some more information on PDDEs can be seen in [4, 20, 21, 38]. Figure 1 shows the studio pantograph model.

Recently, various numerical and analytical approaches have been developed to solve MPDDEs. Some studies were proposed to solve some classes of MPDDEs such as fractional and fractal-fractional DDEs such as spectral methods, collocation methods, operational matrices, etc. Researchers have employed the homotopy analysis and residual power series techniques to solve the DDEs [16]. A spectral method was described to solve the nonlinear FDDEs in [17]. A collocation approach is introduced to solve nonlinear fractional DDEs in [31]. A wavelet and operational matrix approaches are introduced in [7, 33] to solve the fractal-fractional DDEs.

Additionally, wavelet theory has witnessed significant expansion across various fields, demonstrating its distinctive capabilities in disciplines such as engineering, mathematics, science, etc [13, 33]. This theory acts as a versatile mathematical tool, facilitating the analysis of a wide range of distinct problems. Numerous applications exist across various domains, encompassing quantum theory, digital image processing, signal analysis, etc. [12, 36]. Wavelet



approaches are preferred by researchers due to their superior precision and beneficial attributes such as compact support, orthogonality, and spectral accuracy, setting them apart from alternative techniques [14, 32, 37]. Wavelet approximation techniques are employed to solve various problems, encompassing PDDEs of integer, fractional, and fractal-fractional order. In this work, we introduce the wavelet technique to solve the MPDDEs with fractal order.

The concept of a fractal operator comprehensively considers the fractal geometry of the dynamic system, along with factors such as heterogeneity, memory effect, and elasto-viscosity of the medium. Due to the novel concept of the fractal operator and its numerous applications across various domains, researchers are currently emphasizing the formulation and numerical simulation of models that incorporate this innovative operator. Considering the ideas presented in the preceding literature review, we introduce a novel approach: numerical study of a FMPDDEs featuring variable coefficients corresponding to the provided Eq.(1.1). The FMPDDEs is achieved through the utilization of fractal differential operators, as defined in Eqs.(1.1) and (1.2). As far as we are aware, there is presently no prior research addressing MPDDEs with involvement of fractal derivatives. Moreover, we provide numerical approximations of the solutions utilizing Jacobi fractional-order wavelets ($J_O^F Ws$). The numerical approach presented relies on the fractal integral operational matrix (FIOM) for $J_O^F Ws$ in conjunction with the collocation method. This approach converts the introduced model into a set of algebraic equations by expressing derivative terms as wavelet series with unspecified coefficients. Subsequently, we computed the unknown wavelet coefficients by utilizing the characteristics of $J_O^F Ws$, in conjunction with collocation points and FIOM, to derive an approximate numerical wavelet solution for the presented model.

The paper is structured as follows: The helpful definitions of fractal calculus and the $J_O^F Ws$ with function approximation can be found in section 2. In section 3, the FIOM of the $J_O^F Ws$ is given. Section 4 presents an approximate solution to the FMPDDEs model using wavelets. We introduce some important criteria in section 5 to evaluate the stability and accuracy of the approximations. Some illustrative numerical examples are provided in section 6 for illustrating the accuracy and effectiveness of the constructed scheme. Lastly, the conclusion and significance are provided in sections 7 and 8.

2. BASIC DEFINITIONS

In this section, we have discussed the fractal operator, Jacobi fractional order wavelet and their properties, which are defined in the following subsections.

2.1. Fractal operator (FO). The fractal derivative and integral operators, with the power-law kernel, are discussed in this subsection.

In a fractal space, consider $\xi(\tau) \in C_\mu[a, b]$ as a fractal continuous function. Then the fractal derivative (FD) of the function $\xi(\tau)$ of order μ can be defined by converting the conventional integer-dimensional space-time (ξ, τ) into integer-dimensional space with fractal time (ξ, τ^μ) , see in [1, 3, 23]

$${}^{FO}\mathfrak{D}_\tau^\mu \xi(\tau) = \frac{d\xi(\tau)}{d\tau^\mu} = \lim_{\tau \rightarrow s} \frac{\xi(\tau) - \xi(s)}{\tau^\mu - s^\mu}, \quad (2.1)$$

where μ denotes the fractal dimension of time.

Furthermore, the FD can be defined by converting the conventional integer-dimensional space-time (ξ, τ) into fractal dimensional space-time (ξ^ν, τ^μ)

$${}^{FO}\mathfrak{D}_\tau^\mu \xi^\nu(\tau) = \frac{d\xi^\nu(\tau)}{d\tau^\mu} = \lim_{\tau \rightarrow s} \frac{\xi^\nu(\tau) - \xi^\nu(s)}{\tau^\mu - s^\mu}, \quad (2.2)$$

where ν denotes the fractal dimension of space.

If for the given function ξ both the classical derivative and FD exist then by using the chain rule, Eqs.(2.1) and (2.2) can be written respectively as

$${}^{FO}\mathfrak{D}_\tau^\mu \xi(\tau) = \frac{1}{\mu} \tau^{1-\mu} \frac{d}{d\tau} \xi(\tau) \quad (2.3)$$



and

$${}^{FO}\mathfrak{D}_\tau^\mu \xi^\nu(\tau) = \frac{\nu}{\mu} \tau^{1-\mu} \xi^{\nu-1}(\tau) \frac{d}{d\tau} \xi(\tau).$$

Let the $\xi(\tau) \in C_\mu[a, b]$, then fractal integral (FI) of the function $\xi(\tau)$ with fractal order μ is given by, see in [1, 3, 23]

$${}^{FO}\mathfrak{I}_\tau^\mu \xi(\tau) = \int_0^\tau \xi(s) ds^\mu. \tag{2.4}$$

If $\xi(\tau) \in C[a, b]$ as well, then the FI defined in Eq.(2.4) can be written as

$${}^{FO}\mathfrak{I}_\tau^\mu \xi(\tau) = \mu \int_0^\tau s^{\mu-1} \xi(s) ds. \tag{2.5}$$

Now, the relation between FD and FI operator is given by

$${}^{FO}\mathfrak{I}_\tau^\mu [{}^{FO}\mathfrak{D}_\tau^\mu \xi(\tau)] = \xi(\tau) - \xi(0). \tag{2.6}$$

Remark 2.1. If $\mu = 1$, then the FD and FI operators defined above will become the classical derivative and integral, respectively.

In the next subsection, the Jacobi fractional order wavelets and their properties are defined.

2.2. Jacobi fractional order wavelets ($J_O^F Ws$). A family of $\phi \psi_{n,m}^{(\alpha,\beta)}$ in $L^2[0, 1]$ over the interval $[0, 1]$ is known as $J_O^F Ws$ and defined by, see in [8, 30]

$$\phi \psi_{n,m}^{(\alpha,\beta)}(\tau) = \begin{cases} \frac{2^{\frac{r-1}{2}}}{\sqrt{\phi \mathfrak{h}_m^{(\alpha,\beta)}}} \phi \mathcal{J}_m^{(\alpha,\beta)}(2^{r-1}\tau - n + 1), & \frac{n-1}{2^{r-1}} \leq \tau < \frac{n}{2^{r-1}}, \\ 0, & \text{elsewhere,} \end{cases} \tag{2.7}$$

where $m = 0, 1, 2, \dots, M - 1$ and $n = 1, 2, \dots, 2^{r-1}$; for $M, r \in \mathbb{Z}^+$. Here, $2^{-(r-1)}$ and $(n - 1)2^{-(r-1)}$ are dilation and translation parameters in the dyadic form, respectively. Also, the coefficient $\frac{1}{\sqrt{\phi \mathfrak{h}_m^{(\alpha,\beta)}}}$ is an orthonormality factor relative to weight function $\phi \rho^{(\alpha,\beta)}(\tau) = \tau^{(\phi\beta+\phi-1)}[1 - \tau^\phi]^\alpha$, and

$$\phi \mathfrak{h}_m^{(\alpha,\beta)} = \frac{\Gamma(\alpha + m + 1)\Gamma(\beta + m + 1)}{(\phi)(2m + 1 + \alpha + \beta)\Gamma(m + 1)\Gamma(\alpha + \beta + m + 1)}.$$

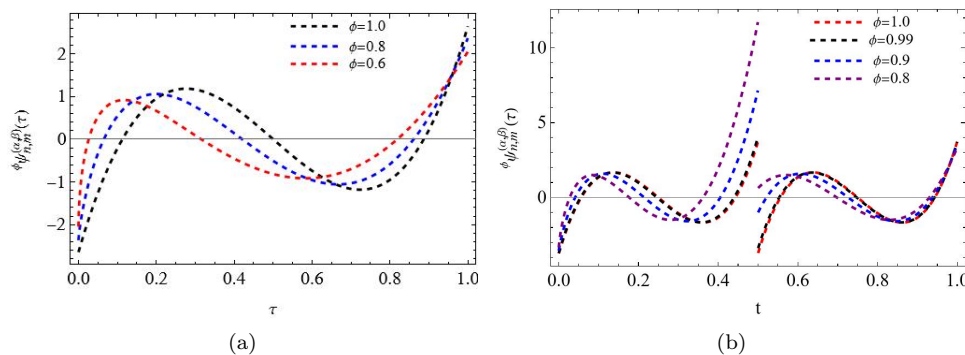


FIGURE 2. Graph depicting $J_O^F Ws$ for various values of ϕ at $\alpha = \beta = 0.5, r = 1$ in 2(a) and at $\alpha = \beta = 0.5, r = 2$ in 2(b) for $m = 3$.



In the preceding Eq. (2.7), $\phi \mathcal{J}_m^{(\alpha,\beta)}(\tau)$ represents the shifted Jacobi fractional order polynomial functions with order $m\phi$, which adhere to the recurrence relation provided below [40]

$$\begin{aligned} \phi \mathcal{J}_0^{(\alpha,\beta)}(\tau) &= 1, \\ \phi \mathcal{J}_1^{(\alpha,\beta)}(\tau) &= (\alpha + 1)(\alpha + \beta + 2)(\tau^\phi - 1), \end{aligned}$$

and

$$\begin{aligned} \phi \mathcal{J}_j^{(\alpha,\beta)}(\tau) &= \frac{(2j + \alpha + \beta - 1)[(2j + \alpha + \beta)(2j + \alpha + \beta - 2)(2\tau^\phi - 1) + \alpha^2 - \beta^2]}{2j(j + \alpha + \beta)(2j + \alpha + \beta - 2)} \phi \mathcal{J}_{j-1}^{(\alpha,\beta)}(\tau) \\ &\quad - \frac{2(j + \alpha - 1)(j + \beta - 1)(2j + \alpha + \beta)}{2j(j + \alpha + \beta)(2j + \alpha + \beta - 2)} \phi \mathcal{J}_{j-2}^{(\alpha,\beta)}(\tau). \end{aligned}$$

Here, $0 < \phi \leq 1$ is the fractional parameter and $\alpha, \beta \geq -1$ are the Jacobi parameter for the wavelets. Also, the $J_O^F W$ s possess finite compact support, i.e.,

$$\text{supp} \left\{ \phi \psi_{n,m}^{(\alpha,\beta)}(\tau) \right\} = \left\{ \tau : \phi \psi_{n,m}^{(\alpha,\beta)}(\tau) \neq 0 \right\} = \left[\frac{n-1}{2^{r-1}}, \frac{n}{2^{r-1}} \right].$$

The system of $J_O^F W$ s mentioned above forms an orthonormal set w.r.t. weight function $\phi \rho_n^{(\alpha,\beta)}(\tau)$ in $L^2[0, 1]$, i.e.,

$$\begin{aligned} \langle \phi \psi_{n,m}^{(\alpha,\beta)}(\tau), \phi \psi_{n',m'}^{(\alpha,\beta)}(\tau) \rangle_{\phi \rho_n^{(\alpha,\beta)}} &= \int_0^1 \left(\phi \psi_{n,m}^{(\alpha,\beta)}(\tau) \phi \psi_{n',m'}^{(\alpha,\beta)}(\tau) \right) \phi \rho_n^{(\alpha,\beta)}(\tau) d\tau \\ &= \begin{cases} 1, & (n, m) = (n', m'), \\ 0, & (n, m) \neq (n', m'), \end{cases} \end{aligned}$$

where the notation $\langle \cdot, \cdot \rangle_{\phi \rho_n^{(\alpha,\beta)}}$ represents the inner product within the space of weighted square-integrable functions, denoted as $L^2_{\phi \rho_n^{(\alpha,\beta)}}[0, 1]$ and $\phi \rho_n^{(\alpha,\beta)}(\tau)$ is defined for the $J_O^F W$ s as

$$\phi \rho_n^{(\alpha,\beta)}(\tau) = \begin{cases} \phi \rho^{(\alpha,\beta)}(2^{r-1}\tau - n + 1), & \frac{n-1}{2^{r-1}} \leq \tau < \frac{n}{2^{r-1}}, \\ 0, & \text{elsewhere.} \end{cases} \tag{2.8}$$

Certain functions are orthonormal only with respect to some weight function in a specified interval. Here, the system of $J_O^F W$ s performs the orthonormality with the weight function $\phi \rho_n^{(\alpha,\beta)}(\tau)$.

Some $J_O^F W$ s for the different values of the fractional parameter ϕ are depicted in Figure 2.

Note: The special cases of $J_O^F W$ s include fractional Legendre wavelets at $\alpha = \beta = 0$, fractional Gegenbauer wavelets at $\alpha = \beta$, fractional Chebyshev wavelets of 1st and 2nd kind at $\alpha = \beta = -\frac{1}{2}$ and $\alpha = \beta = \frac{1}{2}$, respectively. In these special cases, $0 < \phi \leq 1$ represents the fractional parameter. Additionally, the $J_O^F W$ s basis becomes the classical Jacobi wavelet basis if $\phi = 1$.

In the subsequent subsection, we utilize the $J_O^F W$ s as a basis to formulate a series approximation for any square integrable function in terms of $J_O^F W$ s.

2.3. Function approximation. A square-integrable function $\Xi(\tau) \in L^2[0, 1] \cap L^2_{\phi \rho_n^{(\alpha,\beta)}}[0, 1]$ can be approximated by a series of $J_O^F W$ s within the interval $[0, 1]$, as follows: see in [33]

$$\Xi(\tau) = \sum_{n=1}^{\infty} \sum_{m=0}^{\infty} c_{n,m} \phi \psi_{n,m}^{(\alpha,\beta)}(\tau), \tag{2.9}$$

where $c_{n,m}$ is the wavelet coefficients and obtained by

$$c_{n,m} = \left\langle \Xi(\tau), \phi \psi_{n,m}^{(\alpha,\beta)}(\tau) \right\rangle_{\phi \rho_n^{(\alpha,\beta)}(\tau)}, \tag{2.10}$$

here, $\langle \cdot, \cdot \rangle_{\phi \rho_n^{(\alpha,\beta)}(\tau)}$ denotes the inner product in $L^2[0, 1]$ with the weight function $\phi \rho_n^{(\alpha,\beta)}(\tau)$ given in Eq. (2.8).



Now, the finite portion of the preceding infinite series is symbolized by $\Xi_{\widehat{m}}(\tau)$ and expressed as;

$$\Xi(\tau) \simeq \sum_{n=1}^{2^{r-1}} \sum_{m=0}^{M-1} c_{n,m} \phi \psi_{n,m}^{(\alpha,\beta)}(\tau) = \Xi_{\widehat{m}}(\tau), \tag{2.11}$$

Moreover, it can be reformulated in vector terms as follows;

$$\Xi_{\widehat{m}}(\tau) = \mathfrak{C}^T \phi \psi^{(\alpha,\beta)}(\tau), \tag{2.12}$$

where \mathfrak{C} and $\phi \psi^{(\alpha,\beta)}(\tau)$ are $\widehat{m} \times 1$ order vectors and defined as

$$\begin{aligned} \mathfrak{C}_{\widehat{m} \times 1} &= [c_{1,0}, \dots, c_{1,M-1}, c_{2,0}, \dots, c_{2,M-1}, \dots, c_{2^{r-1},0}, \dots, c_{2^{r-1},M-1}]^T \\ &= [c_1, c_2, c_3, \dots, c_{\widehat{m}}]^T, \end{aligned} \tag{2.13}$$

and

$$\begin{aligned} \phi \psi_{\widehat{m} \times 1}^{(\alpha,\beta)}(\tau) &= [\phi \psi_{1,0}^{(\alpha,\beta)}(\tau), \dots, \phi \psi_{1,M-1}^{(\alpha,\beta)}(\tau), \phi \psi_{2,0}^{(\alpha,\beta)}(\tau), \dots, \phi \psi_{2,M-1}^{(\alpha,\beta)}(\tau), \dots, \phi \psi_{2^{r-1},0}^{(\alpha,\beta)}(\tau), \dots, \phi \psi_{2^{r-1},M-1}^{(\alpha,\beta)}(\tau)]^T \\ &= [\phi \psi_1^{(\alpha,\beta)}, \phi \psi_2^{(\alpha,\beta)}, \phi \psi_3^{(\alpha,\beta)}, \dots, \phi \psi_{\widehat{m}}^{(\alpha,\beta)}]^T. \end{aligned} \tag{2.14}$$

In this context, $\widehat{m} = 2^{r-1}M$ represents the total number of basis functions for $J_{\mathcal{O}}^F Ws$ and T signifies the conventional transpose operation applied to the vector.

2.4. Example: Approximation of fractal function in terms of $J_{\mathcal{O}}^F Ws$. In this work, we introduced the concept of the fractal derivative to develop a fractal model of differential equations. It is clear that the fractal derivative of a fractal function can be determined using Eqs. (2.1) and (2.2), whereas the classical derivative of these fractal functions does not exist. Additionally, for a continuous function, for which both the classical derivative and the fractal derivative exist, the fractal derivative can be found using Eq. (2.3).

$$\Xi(\tau) = \begin{cases} \frac{9\tau}{4}, & 0 \leq \tau \leq \frac{1}{9}, \\ \frac{1}{4}, & \frac{1}{9} < \tau \leq \frac{2}{9}, \\ \frac{1}{4}(9\tau - 1), & \frac{2}{9} < \tau \leq \frac{1}{3}, \\ \frac{1}{2}, & \frac{1}{3} < \tau \leq \frac{2}{3}, \\ \frac{9\tau}{4} - 1, & \frac{2}{3} < \tau \leq \frac{7}{9}, \\ \frac{3}{4}, & \frac{7}{9} < \tau \leq \frac{8}{9}, \\ \frac{1}{4}(9\tau - 5), & \frac{8}{9} < \tau \leq 1, \\ 0, & \text{elsewhere.} \end{cases} \tag{2.15}$$

Moreover, we have considered the cantor-type function defined in Eq. (2.15) which is the well known example of a fractal function for which the fractal derivative exists while the classical derivative does not. This cantor type fractal function $\Xi(\tau)$ was approximated using the wavelet technique. The exact graph and wavelets approximated graph of this cantor type fractal function $\Xi(\tau)$ are shown in Figure 3, which indicates that the approximation of the fractal function in terms of continuous wavelets is a smooth function.

In the subsequent section, we construct the operational matrix of $J_{\mathcal{O}}^F Ws$ for fractal integration, which will be employed in solving problems related to fractal MPDDEs.

3. FRACTAL INTEGRAL OPERATIONAL MATRIX (FIOM)

The FIOM of $J_{\mathcal{O}}^F Ws$ with order $\widehat{m} \times \widehat{m}$ is denoted by ${}_{\mu} \mathfrak{M}_{\widehat{m} \times \widehat{m}}^{(\alpha,\beta)}$ and defined as;

$$\int_0^{\tau} \frac{\phi \psi_{\widehat{m} \times 1}^{(\alpha,\beta)}(s)}{s^{(1-\mu)}} ds \simeq {}_{\mu} \mathfrak{M}_{\widehat{m} \times \widehat{m}}^{(\alpha,\beta)} \phi \psi_{\widehat{m} \times 1}^{(\alpha,\beta)}(\tau), \tag{3.1}$$



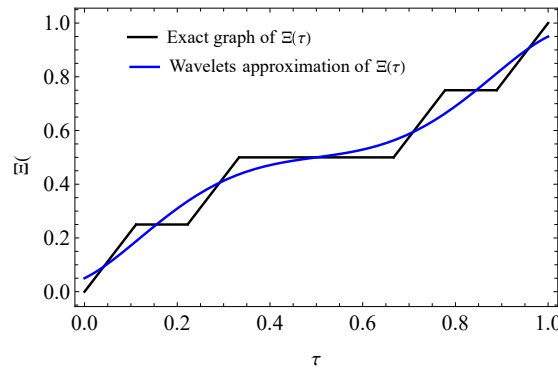


FIGURE 3. The figure shows the graph of exact values of $\Xi(\tau)$ and wavelet approximated values of $\Xi(\tau)$.

where, $\phi\psi_{\widehat{m}\times\widehat{m}}^{(\alpha,\beta)}(\tau)$ is defined in Eq. (2.14) and the $\phi\mathfrak{M}_{\widehat{m}\times\widehat{m}}^{(\alpha,\beta)}$ is determined by

$$\phi\mathfrak{M}_{\widehat{m}\times\widehat{m}}^{(\alpha,\beta)} = \left\langle \phi\mathcal{I}_{\widehat{m}\times\widehat{m}}^{(\alpha,\beta)}(\tau), [\phi\psi_{\widehat{m}\times\widehat{m}}^{(\alpha,\beta)}(\tau)]^T \right\rangle_{\phi\rho_n^{(\alpha,\beta)}(\tau)}, \tag{3.2}$$

here, $\phi\mathcal{I}_{\widehat{m}\times\widehat{m}}^{(\alpha,\beta)}(\tau)$ is defined as,

$$\begin{aligned} \phi\mathcal{I}_{\widehat{m}\times\widehat{m}}^{(\alpha,\beta)}(\tau) &= \int_0^\tau \frac{\phi\psi_{\widehat{m}\times\widehat{m}}^{(\alpha,\beta)}(s)}{s^{(1-\mu)}} ds \\ &= \left[\phi\mathcal{I}_{1,0}^{(\alpha,\beta)}(\tau), \phi\mathcal{I}_{1,1}^{(\alpha,\beta)}(\tau), \dots, \phi\mathcal{I}_{2^{r-1},M-1}^{(\alpha,\beta)}(\tau) \right]_{1\times 2^{r-1}M}^T, \end{aligned} \tag{3.3}$$

where,

$$\phi\mathcal{I}_{2^{r-1},(M-1)}^{(\alpha,\beta)}(\tau) = \int_0^\tau s^{(\mu-1)} \phi\psi_{2^{r-1},M-1}^{(\alpha,\beta)}(s) ds, \quad \text{for } r, M \in \mathbb{Z}^+.$$

Note: The fractal derivative and integral defined in Eqs. (2.3) and (2.5), are used in this work. In the subsequent section, we have developed the wavelet approach to solve the considered model.

4. THE WAVELET APPROACH FOR SOLVING THE FMPDDEs MODEL WITH VARYING COEFFICIENTS

In this part, we develop an efficient wavelet collocation technique for solving FMPDDEs models, which follows below in description.

To estimate the numerical solution of the provided FMPDDEs model in Eq. (1.2), we begin by approximating the unknown FD term ${}^{FO}\mathcal{D}_t^\mu \xi(t)$ (see in Eq. (2.3)) utilizing the $J_O^F Ws$ series within the interval $[0, 1)$ (also see Eq. (2.9)), we obtain

$${}^{FO}\mathcal{D}_t^\mu \xi(t) \simeq \mathfrak{C}_{\widehat{m}\times\widehat{m}}^T \phi\psi_{\widehat{m}\times\widehat{m}}^{(\alpha,\beta)}(t) = {}^{FO}\mathcal{D}_t^\mu \xi_{\widehat{m}}(t), \tag{4.1}$$

where the finite portion of the $J_O^F Ws$ series for the derivative ${}^{FO}\mathcal{D}_t^\mu \xi(t)$ is denoted by ${}^{FO}\mathcal{D}_t^\mu \xi_{\widehat{m}}(t)$ according to Eq. (2.11). The vectors $\mathfrak{C}_{\widehat{m}\times\widehat{m}}^T$ and $\phi\psi_{\widehat{m}\times\widehat{m}}^{(\alpha,\beta)}(t)$ are defined similarly as Eqs. (2.13) and (2.14) respectively.

Now, Applying the FI operator provided in Eq. (2.5) to both sides of Eq. (4.1), we obtain

$${}^{FO}\mathcal{J}_t^\mu ({}^{FO}\mathcal{D}_t^\mu \xi(t)) \simeq {}^{FO}\mathcal{J}_t^\mu \left(\mathfrak{C}_{\widehat{m}\times\widehat{m}}^T \phi\psi_{\widehat{m}\times\widehat{m}}^{(\alpha,\beta)}(t) \right).$$

So, the above expression suggests that

$$({}^{FO}\mathcal{J}_t^\mu {}^{FO}\mathcal{D}_t^\mu) \xi(t) \simeq \mathfrak{C}_{\widehat{m}\times\widehat{m}}^T \left({}^{FO}\mathcal{J}_t^\mu \phi\psi_{\widehat{m}\times\widehat{m}}^{(\alpha,\beta)}(t) \right),$$



using Eqs. (2.5) and (2.6), we have

$$\xi(t) - \xi(0) \simeq \mu \mathbf{e}_{\widehat{m} \times 1}^T \int_0^t (s)^{\mu-1} \phi \psi_{\widehat{m} \times 1}^{(\alpha, \beta)}(s) ds. \tag{4.2}$$

Now, using Eq. (3.1), it yields

$$\xi(t) - \xi(0) \simeq \mu \mathbf{e}_{\widehat{m} \times 1}^T \mu \mathfrak{M}_{\widehat{m} \times \widehat{m}}^{(\alpha, \beta)} \phi \psi_{\widehat{m} \times 1}^{(\alpha, \beta)}(t).$$

Here, $\mu \mathfrak{M}_{\widehat{m} \times \widehat{m}}^{(\alpha, \beta)}$ represents the FIOM of order $\widehat{m} \times \widehat{m}$, as defined in Eq. (3.2).

Next, we use Eq. (2.11) to simplify and apply the initial condition, such as

$$\xi(t) \simeq \mu \mathbf{e}_{\widehat{m} \times 1}^T \mu \mathfrak{M}_{\widehat{m} \times \widehat{m}}^{(\alpha, \beta)} \phi \psi_{\widehat{m} \times 1}^{(\alpha, \beta)}(t) + \xi_0 = \xi_{\widehat{m}}(t). \tag{4.3}$$

Similarly as above, the delay function $\xi(k_i t)$ in Eq. (1.2) can be obtained as

$$\xi(k_i t) \simeq \mu \mathbf{e}_{\widehat{m} \times 1}^T \mu \mathfrak{M}_{\widehat{m} \times \widehat{m}}^{(\alpha, \beta)} \phi \psi_{\widehat{m} \times 1}^{(\alpha, \beta)}(k_i t) + \xi_0 = \xi_{\widehat{m}}(k_i t). \tag{4.4}$$

Next, we substitute Eqs. (4.1), (4.3), and (4.4) into the Eq.(1.2), we derive;

$$\begin{aligned} \mathbf{e}_{\widehat{m} \times 1}^T \phi \psi_{\widehat{m} \times 1}^{(\alpha, \beta)}(t) &= p(t) \left(\mu \mathbf{e}_{\widehat{m} \times 1}^T \mu \mathfrak{M}_{\widehat{m} \times \widehat{m}}^{(\alpha, \beta)} \phi \psi_{\widehat{m} \times 1}^{(\alpha, \beta)}(t) + \xi_0 \right) \\ &+ \sum_{i=1}^l q_i(t) \left(\mu \mathbf{e}_{\widehat{m} \times 1}^T \mu \mathfrak{M}_{\widehat{m} \times \widehat{m}}^{(\alpha, \beta)} \phi \psi_{\widehat{m} \times 1}^{(\alpha, \beta)}(k_i t) + \xi_0 \right) + F(t). \end{aligned} \tag{4.5}$$

In this manner, we collocate the above system Eq. (4.5) at the appropriate collocation points t_j , as follows:

$$\begin{aligned} \mathbf{e}_{\widehat{m} \times 1}^T \phi \psi_{\widehat{m} \times 1}^{(\alpha, \beta)}(t_j) &= p(t_j) \left(\mu \mathbf{e}_{\widehat{m} \times 1}^T \mu \mathfrak{M}_{\widehat{m} \times \widehat{m}}^{(\alpha, \beta)} \phi \psi_{\widehat{m} \times 1}^{(\alpha, \beta)}(t_j) + \xi_0 \right) \\ &+ \sum_{i=1}^l q_i(t_j) \left(\mu \mathbf{e}_{\widehat{m} \times 1}^T \mu \mathfrak{M}_{\widehat{m} \times \widehat{m}}^{(\alpha, \beta)} \phi \psi_{\widehat{m} \times 1}^{(\alpha, \beta)}(k_i t_j) + \xi_0 \right) + F(t_j), \end{aligned} \tag{4.6}$$

where, $t_j = \frac{j-0.9}{\widehat{m}}$; $j = 1, 2, \dots, \widehat{m}$. Therefore, simplifying Eq. (4.6) yields a transformed algebraic system of equations, as follows

$$\mathfrak{P}_{\widehat{m} \times \widehat{m}} \mathbf{e}_{\widehat{m} \times 1} = \mathfrak{F}_{\widehat{m} \times 1}, \tag{4.7}$$

here,

$$\mathfrak{P}_{\widehat{m} \times \widehat{m}} = [\mathfrak{P}_{t_1}^T, \mathfrak{P}_{t_2}^T, \dots, \mathfrak{P}_{t_j}^T, \dots, \mathfrak{P}_{t_{\widehat{m}}}^T]^T,$$

with the matrix of order $\widehat{m} \times 1$

$$\mathfrak{P}_{t_j} = \phi \psi_{\widehat{m} \times 1}^{(\alpha, \beta)}(t_j) - p(t_j) \left(\mu \mathfrak{M}_{\widehat{m} \times \widehat{m}}^{(\alpha, \beta)} \phi \psi_{\widehat{m} \times 1}^{(\alpha, \beta)}(t_j) \right) - \sum_{i=1}^l q_i(t_j) \left(\mu \mathfrak{M}_{\widehat{m} \times \widehat{m}}^{(\alpha, \beta)} \phi \psi_{\widehat{m} \times 1}^{(\alpha, \beta)}(k_i t_j) \right),$$

and

$$\mathfrak{F}_{\widehat{m} \times 1} = [\mathfrak{F}_{t_1}, \mathfrak{F}_{t_2}, \dots, \mathfrak{F}_{t_j}, \dots, \mathfrak{F}_{t_{\widehat{m}}}]^T,$$

with

$$\mathfrak{F}_{t_j} = F(t_j) + \xi_0 \left(p(t_j) + \sum_{i=1}^l q_i(t_j) \right),$$

here \mathfrak{F}_{t_j} is the order of 1×1 matrix at t_j .

The system derived in Eq. (4.7) can now be efficiently solved for the unknown wavelet coefficients vector \mathbf{e} utilizing the computational software Mathematica 13.1. Ultimately, we use Eq. (4.3) and the coefficients vector \mathbf{e} to find an effective approximate numerical solution for the model under consideration.

The process of the constructed method is expressed as follows:



Pseudo-code for the solution of FMPDDEs:

Input: Introduce $n = 1, 2, \dots, 2^{r-1}$, $m = 0, 1, 2, \dots, M - 1$, $\widehat{m} = 2^{r-1}M$; $r, M \in \mathbb{Z}^+$, $0 < \phi \leq 1$, $0 < \mu \leq 1$, $\alpha, \beta \geq -1$, $0 < k_i < 1$.

Step 1: Consider $J_O^F Ws$ as $\phi \psi_{\widehat{m} \times 1}^{(\alpha, \beta)}(t) = [\phi \psi_1^{(\alpha, \beta)}, \phi \psi_2^{(\alpha, \beta)}, \phi \psi_3^{(\alpha, \beta)}, \dots, \phi \psi_{\widehat{m}}^{(\alpha, \beta)}]^T$. (see Eq.(2.14)).

Step 2: Introduce the unknown vector \mathfrak{C} such as $\mathfrak{C}_{\widehat{m} \times 1} = [c_1, c_2, c_3, \dots, c_{\widehat{m}}]^T$ (see Eq.(2.13)).

Step 3: Utilizing **Steps 1** and **2**, approximate ${}^{FO}\mathfrak{D}_t^\mu \xi(t)$ in terms of the $J_O^F Ws$ as ${}^{FO}\mathfrak{D}_t^\mu \xi(t) \simeq \mathfrak{C}_{\widehat{m} \times 1}^T \phi \psi_{\widehat{m} \times 1}^{(\alpha, \beta)}(t) = {}^{FO}\mathfrak{D}_t^\mu \xi_{\widehat{m}}(t)$. (see Eq.(4.1)).

Step 4: Compute the FIOM $\phi \mathfrak{M}_{\widehat{m} \times \widehat{m}}^{(\alpha, \beta)} = \int_0^1 \left(\phi \mathcal{I}_{\widehat{m} \times 1}^{(\alpha, \beta)}(t) \phi \psi_{1 \times \widehat{m}}^{(\alpha, \beta)}(t) \right) \phi \rho_n^{(\alpha, \beta)}(t) dt$, (see Eq.(3.2)).

Step 5: Using **Steps 3** and **4**, compute the approximate $\xi(t)$ such as $\xi(t) \simeq \mu \mathfrak{C}_{\widehat{m} \times 1}^T \phi \mathfrak{M}_{\widehat{m} \times \widehat{m}}^{(\alpha, \beta)} \phi \psi_{\widehat{m} \times 1}^{(\alpha, \beta)}(t) + \xi_0 = \xi_{\widehat{m}}(t)$ (see Eq.(4.3)).

Step 6: Also, calculate the delay function $\xi(k_i t)$ by substituting $t \rightarrow k_i t$ in the result of **Step 5** as $\xi(k_i t) \simeq \mu \mathfrak{C}_{\widehat{m} \times 1}^T \phi \mathfrak{M}_{\widehat{m} \times \widehat{m}}^{(\alpha, \beta)} \phi \psi_{\widehat{m} \times 1}^{(\alpha, \beta)}(k_i t) + \xi_0 = \xi_{\widehat{m}}(k_i t)$. (see Eq.(4.4)).

Step 7: Consider to **Steps 3, 5** and **6**, compute the FMPDDEs ${}^{FO}\mathfrak{D}_t^\mu \xi(t) = p(t)\xi(t) + \sum_{i=1}^l q_i(t)\xi(k_i t) + F(t)$; $0 < t \leq 1$ with the initial condition $\xi(0) = \xi_0$.

Step 8: Next, by collocating the output from **Step 7** at the collocation nodes $t_j = \frac{j-0.9}{\widehat{m}}$ for $j = 1, 2, \dots, \widehat{m}$, we obtain the system of algebraic equations.

Step 9: To determine the value of \mathfrak{C} , solve the system of equations acquired in **Step 8**.

Output: The approximate solution using wavelets;

$$\xi(t) \simeq \mu \mathfrak{C}_{\widehat{m} \times 1}^T \phi \mathfrak{M}_{\widehat{m} \times \widehat{m}}^{(\alpha, \beta)} \phi \psi_{\widehat{m} \times 1}^{(\alpha, \beta)}(t) + \xi_0.$$

5. ANALYSIS OF STABILITY AND ERRORS

This section addresses essential aspects of evaluating the stability of the developed method as well as the error analysis of the numerical solutions in the following two subsections.

Stability analysis.

Lemma 5.1. [22] Assuming $\xi \in L_{\phi \rho^{(\alpha, \beta)}}^2(I)$ be a square integrable function defined on the interval I and the completeness of the system $\{\phi \psi_{n, m}^{(\alpha, \beta)}\}_{n, m \in \mathbb{Z}}$ in $L_{\phi \rho^{(\alpha, \beta)}}^2(I)$, it follows that the $J_O^F Ws$ coefficient $c_{n, m}$ is bounded, i.e.,

$$|c_{n, m}| \leq \|\xi\|_{\phi \rho^{(\alpha, \beta)}} \left\| \phi \psi_{n, m}^{(\alpha, \beta)} \right\|_{\phi \rho^{(\alpha, \beta)}}.$$

Additionally, the $J_O^F Ws$ system is also a frame, i.e.,

$$\mathcal{A} \|\xi\|_{\phi \rho^{(\alpha, \beta)}}^2 \leq \sum_{n, m \in \mathbb{Z}} \left| \left\langle \xi, \phi \psi_{n, m}^{(\alpha, \beta)} \right\rangle_{\phi \rho^{(\alpha, \beta)}} \right|^2 \leq \mathcal{B} \|\xi\|_{\phi \rho^{(\alpha, \beta)}}^2,$$

where $0 < \mathcal{A} \leq \mathcal{B} < \infty$ are certain constants.

Proof. Consider $\xi \in L_{\phi \rho^{(\alpha, \beta)}}^2(I)$ and $\phi \psi_{n, m}^{(\alpha, \beta)} \in L_{\phi \rho^{(\alpha, \beta)}}^2(I)$, then utilizing the Eq. (2.10) and Schwarz's inequality, such as

$$\begin{aligned} |c_{n, m}| &= \left| \left\langle \xi, \phi \psi_{n, m}^{(\alpha, \beta)} \right\rangle_{\phi \rho^{(\alpha, \beta)}} \right| \\ &= \left| \int_I \xi(t) \phi \psi_{n, m}^{(\alpha, \beta)}(t) \phi \rho^{(\alpha, \beta)}(t) dt \right| \\ &\leq \left(\int_I |\xi(t)|^2 \phi \rho^{(\alpha, \beta)}(t) dt \right)^{\frac{1}{2}} \left(\int_I \left| \phi \psi_{n, m}^{(\alpha, \beta)}(t) \right|^2 \phi \rho^{(\alpha, \beta)}(t) dt \right)^{\frac{1}{2}} \\ &\leq \|\xi\|_{\phi \rho^{(\alpha, \beta)}} \left\| \phi \psi_{n, m}^{(\alpha, \beta)} \right\|_{\phi \rho^{(\alpha, \beta)}}. \end{aligned} \tag{5.1}$$



Further, the second part of the proof for this theorem is available in [22]. □

Theorem 5.2. (Existence of a numerical solution): Assuming the completeness of $J_O^F Ws$ system $\{\phi\psi_{n,m}^{(\alpha,\beta)}\}_{n,m \in \mathbb{Z}}$ in $L_{\phi\rho}^2(\alpha,\beta)(I)$, the suggested approach described in section 4 gives an approximate numerical solution if rank of the matrix $\mathfrak{P}_{\widehat{m} \times \widehat{m}}$ and augmented matrix $[\mathfrak{P}_{\widehat{m} \times \widehat{m}} : \mathfrak{F}_{\widehat{m} \times 1}]$ are same for the system considered in Eq. (4.7).

Proof. In the provided hypothesis, the aim is to establish the existence of approximate numerical solutions for the algebraic system described in Eq. (4.7).

Initially, we must ascertain the consistency (stability) of the system. In this sequence, we are verifying the stability of the current algebraic systems alongside their approximate numerical solutions through the following two cases, such as

Case 1: If the rank of the matrices $\mathfrak{P}_{\widehat{m} \times \widehat{m}}$ and $[\mathfrak{P}_{\widehat{m} \times \widehat{m}} : \mathfrak{F}_{\widehat{m} \times 1}]$ are same, i.e.,

$$\text{rank}(\mathfrak{P}_{\widehat{m} \times \widehat{m}}) = \text{rank}([\mathfrak{P}_{\widehat{m} \times \widehat{m}} : \mathfrak{F}_{\widehat{m} \times 1}]), \tag{5.2}$$

consequently, it's a consistent system (stable) and numerical solution exists. Additionally, two subcases arise, as follows

Subcase 1: If the obtained rank is \widehat{m} of the Eq. (5.2), then $\mathfrak{P}_{\widehat{m} \times \widehat{m}}$ matrix is non-singular and its inverse always exists (says, $\mathfrak{P}_{\widehat{m} \times \widehat{m}}^{-1}$) and we have a unique solution. Hence, the solution to the algebraic system described in Eq. (4.7) can be derived as follows,

$$\mathfrak{C} = \mathfrak{P}_{\widehat{m} \times \widehat{m}}^{-1} \mathfrak{F}_{\widehat{m} \times 1}.$$

Subcase 2: If the obtained rank is less than \widehat{m} in Eq. (5.2), then we have an infinite number of solution and these solutions can be obtained using the Gaussian elimination algorithm. Hence, the numerical solution exists to the proposed method.

Case 2: If rank of the matrices $\mathfrak{P}_{\widehat{m} \times \widehat{m}}$ and $[\mathfrak{P}_{\widehat{m} \times \widehat{m}} : \mathfrak{F}_{\widehat{m} \times 1}]$ are not the same, i.e.,

$$\text{rank}(\mathfrak{P}_{\widehat{m} \times \widehat{m}}) \neq \text{rank}([\mathfrak{P}_{\widehat{m} \times \widehat{m}} : \mathfrak{F}_{\widehat{m} \times 1}]),$$

consequently, it's an inconsistent system (unstable) and numerical solution doesn't exist for the proposed method. □

Error analysis. This subsection examines the criteria for convergence and error analysis of the solutions obtained using the methods proposed in Section 4.

[1] : The absolute error function $\mathcal{E}_{abs}(t)$ obtained as

$$\mathcal{E}_{abs}(t) = |\xi(t) - \xi_{\widehat{m}}(t)|; \quad t \in [0, 1], \tag{5.3}$$

where $\xi(t)$ and $\xi_{\widehat{m}}(t)$ represent the exact solution and approximate solution for the considered problem.

[2] : The maximum absolute error \mathcal{E}_{∞} calculated as

$$\mathcal{E}_{\infty} = \max_{t \in [0,1]} |\xi(t) - \xi_{\widehat{m}}(t)|. \tag{5.4}$$

[3] : The L^2 - norm error is determined by

$$\mathcal{E}(t) = \|\xi(t) - \xi_{\widehat{m}}(t)\|; \quad t \in [0, 1]. \tag{5.5}$$

[4] : If the exact solution of the model equation is unknown, the reliability and accuracy of the method can be assessed through the residual error function, given by

$$\mathcal{E}_{\widehat{m}}(t_j) = \left| {}^{FO}\mathfrak{D}_t^{\mu} \xi_{\widehat{m}}(t_j) - \{p(t_j)\xi_{\widehat{m}}(t_j) + \sum_{i=1}^l q_i(t_j)\xi_{\widehat{m}}(\lambda_i t_j) + F(t_j)\} \right|, \tag{5.6}$$

where $t_j \in [0, 1], j = 0, 1, 2, \dots$

Additionally, $\mathcal{E}_{\widehat{m}}(t_j) \rightarrow 0$ implies error decreases.

Furthermore, essential lemmas and theorems are described to facilitate the analysis of the convergence of the method under consideration.



Lemma 5.3. [8] Let $\mathfrak{D}^{i\phi}\xi \in C[0, 1]$ and $(2M+\beta+1)\phi > 0$ for $i = 0, 1, 2, \dots, M-1$, and space $W_{\widehat{m}} = \text{span}\{\phi \mathcal{J}_0^{(\alpha,\beta)}, \phi \mathcal{J}_1^{(\alpha,\beta)}, \dots, \phi \mathcal{J}_{M-1}^{(\alpha,\beta)}\}$. Suppose the best approximation of $\xi(t)$ is $\xi_{\widehat{m}}(t) = B^T \phi \psi^{(\alpha,\beta)}(t)$ in $W_{\widehat{m}}$ with error function $\mathcal{E}_b(t) = \xi(t) - B^T \phi \psi^{(\alpha,\beta)}(t)$ then in the interval $[0, 1]$, the expected solution's error bound will be

$$\|\mathcal{E}_b\|_{\phi\rho^{(\alpha,\beta)}} \leq \eta \|\mathcal{E}_b^2\|^{\frac{1}{2}} \quad \text{and} \quad \|\mathcal{E}_b\| \leq \frac{\mathfrak{L}_\phi}{\Gamma(M\phi + 1)} \frac{1}{\sqrt{(1 + 2M\phi)}},$$

where $\phi \mathcal{J}_{M-1}^{(\alpha,\beta)}$ is defined in subsection 2.2 and

$$\mathfrak{L}_\phi \geq \text{Sup}_{t \in (0,1]} |\mathfrak{D}^{M\phi}\xi(t)|; \quad \eta = \left(\frac{\Gamma(1 + 2\alpha)\Gamma(2 + 2\beta - \frac{1}{\phi})}{\phi\Gamma(3 + 2\alpha + 2\beta - \frac{1}{\phi})} \right)^{\frac{1}{4}}.$$

Proof. Considering the function $\xi_{\widehat{m}}(t)$ in $W_{\widehat{m}}$, we formulate the generalized Taylor's formula as follows:

$$\xi_{\widehat{m}}(t) = \sum_{i=0}^{M-1} \frac{t^{i\phi}}{\Gamma(i\phi + 1)} \mathfrak{D}^{i\phi}\xi(0^+),$$

thus, for every function in the space $W_{\widehat{m}}$ of order $(M-1)\phi$ defined as $\xi_{\widehat{m}}(t) = P^T \phi \mathcal{J}^{(\alpha,\beta)}(t)$, we obtain

$$\begin{aligned} \left| \xi(t) - P^T \phi \mathcal{J}^{(\alpha,\beta)}(t) \right| &= \left| \xi(t) - \sum_{i=0}^{M-1} \frac{t^{i\phi}}{\Gamma(i\phi + 1)} \mathfrak{D}^{i\phi}\xi(0^+) \right| \\ &\leq \frac{t^{M\phi}}{\Gamma(M\phi + 1)} \text{sup}_{t \in (0,1]} |\mathfrak{D}^{M\phi}\xi(0^+)| \\ &\leq \frac{t^{M\phi}}{\Gamma(M\phi + 1)} \mathfrak{L}_\phi, \end{aligned}$$

where $\mathfrak{L}_\phi \geq \text{Sup}_{t \in [0,1]} |\mathfrak{D}^{M\phi}\xi(t)|$. Since $\xi_{\widehat{m}}(t)$ is the best approximation to $\xi(t)$ in $W_{\widehat{m}}$ for the system of $J_O^F W_s$, thus we obtain

$$\begin{aligned} \|\mathcal{E}_b\|^2 &= \left\| \xi(t) - B^T \phi \psi^{(\alpha,\beta)}(t) \right\|^2 \\ &= \left\| \xi(t) - P^T \phi \mathcal{J}^{(\alpha,\beta)}(t) \right\|^2 \\ &\leq \frac{\mathcal{L}_\phi^2}{[\Gamma(M\phi + 1)]^2} \int_0^1 t^{2M\phi} dt \\ &\leq \frac{\mathcal{L}_\phi^2}{[\Gamma(M\phi + 1)]^2} \frac{1}{(1 + 2M\phi)}. \end{aligned}$$

Next, we compute the square roots of both sides to determine the upper error bound. i.e.,

$$\|\mathcal{E}_b\|_2 \leq \frac{\mathfrak{L}_\phi}{\Gamma(M\phi + 1)} \frac{1}{\sqrt{(1 + 2M\phi)}}. \quad (5.7)$$



Moreover, utilizing the properties of norms and Schwarz’s inequality, we determine the approximate solution’s error bound w.r.t. $L^2[0, 1) \cap L^2_{\rho^{(\phi, \alpha, \beta)}}[0, 1)$

$$\begin{aligned} \|\mathcal{E}_b\|_{\phi_{\rho^{(\alpha, \beta)}}}^2 &= \|\xi - \xi_{\widehat{m}}\|_{\phi_{\rho^{(\alpha, \beta)}}}^2 \\ &= \int_0^1 |\xi(t) - \xi_{\widehat{m}}(t)|^2 \phi_{\rho^{(\alpha, \beta)}}(t) dt \\ &\leq \left(\int_0^1 (|\xi(t) - \xi_{\widehat{m}}(t)|^2)^2 dt \right)^{\frac{1}{2}} \left(\int_0^1 (\rho^{(\phi, \alpha, \beta)}(t))^2 dt \right)^{\frac{1}{2}} \\ &\leq \left(\frac{\Gamma(1 + 2\alpha)\Gamma(2 + 2\beta - \frac{1}{\phi})}{\phi\Gamma(3 + 2\alpha + 2\beta - \frac{1}{\phi})} \right)^{\frac{1}{2}} \|(\xi(t) - \xi_{\widehat{m}}(t))^2\|. \end{aligned}$$

Now, by taking the square root of each sides of the previous equation, we obtain

$$\|\mathcal{E}_b\|_{\phi_{\rho^{(\alpha, \beta)}}} \leq \eta \|\mathcal{E}_b^2\|^{\frac{1}{2}}, \tag{5.8}$$

where $\eta = \left(\frac{\Gamma(1+2\alpha)\Gamma(2+2\beta-\frac{1}{\phi})}{\phi\Gamma(3+2\alpha+2\beta-\frac{1}{\phi})} \right)^{\frac{1}{4}}$ and $\phi_{\rho^{(\alpha, \beta)}}(t)$ is weight function for $J_O^F Ws$ provided in subsection 2.2.

As M approaches infinity, the condition $\|\mathcal{E}_b\| \rightarrow 0$ implies that $\|\mathcal{E}_b\|_{\phi_{\rho^{(\alpha, \beta)}}} \rightarrow 0$.

i.e., $\|\mathcal{E}_b\|_{\phi_{\rho^{(\alpha, \beta)}}} \rightarrow 0$ converges more rapidly in comparison to $\|\mathcal{E}_b\| \rightarrow 0$ as $M \rightarrow \infty$. □

Lemma 5.4. *If Lemma 5.3 holds, then we obtain the following inequality:*

$$\|{}^{FO}\mathfrak{J}_t^\mu \xi(t) - {}^{FO}\mathfrak{J}_t^\mu \xi_{\widehat{m}}(t)\| \leq \kappa \|\mathcal{E}_b\|$$

where,

$$0 < \mu \leq 1 \quad \text{and} \quad \kappa = \frac{\mu}{\sqrt{2\mu(2\mu - 1)}}.$$

Proof. Utilizing Eq. (2.5) and Schwarz’s inequality, we obtain

$$\begin{aligned} |{}^{FO}\mathfrak{J}_t^\mu \xi(t) - {}^{FO}\mathfrak{J}_t^\mu \xi_{\widehat{m}}(t)| &\leq \mu \int_0^t (s)^{\mu-1} |\xi(s) - \xi_{\widehat{m}}(s)| ds \\ &\leq \mu \left(\int_0^t (s)^{2\mu-2} ds \right)^{\frac{1}{2}} \left(\int_0^t (\xi(s) - \xi_{\widehat{m}}(s))^2 ds \right)^{\frac{1}{2}} \\ &\leq \frac{\mu}{\sqrt{(2\mu - 1)}} t^{\mu-\frac{1}{2}} \|\mathcal{E}_b\|. \end{aligned} \tag{5.9}$$

Now, if we compute L^2 -norm on both sides of Eq. (5.9), we have the desired result as:

$$\begin{aligned} \|{}^{FO}\mathfrak{J}_t^\mu \xi(t) - {}^{FO}\mathfrak{J}_t^\mu \xi_{\widehat{m}}(t)\| &\leq \frac{\mu}{\sqrt{(2\mu - 1)}} \|t^{\mu-\frac{1}{2}}\| \|\mathcal{E}_b\| \\ &\leq \frac{\mu}{\sqrt{2\mu(2\mu - 1)}} \|\mathcal{E}_b\| \\ &\leq \kappa \|\mathcal{E}_b\|. \end{aligned} \tag{5.10}$$

Additionally, utilizing Lemma 5.3, we get

$$\lim_{M \rightarrow \infty} \|{}^{FO}\mathfrak{J}_t^\mu \xi(t) - {}^{FO}\mathfrak{J}_t^\mu \xi_{\widehat{m}}(t)\| = 0.$$

Similarly, the subsequent inequality holds true:

$$\|{}^{FO}\mathfrak{D}_t^\mu \xi(t) - {}^{FO}\mathfrak{D}_t^\mu \xi_{\widehat{m}}(t)\| \leq \kappa_1 \|\mathcal{E}_b\|, \tag{5.11}$$

where κ_1 is a constant, which depends on μ as similar to κ . □



Next, the convergence of our approximation results is demonstrated by establishing the error bound of the established approach in the following theorem.

Theorem 5.5. *If the derivative ${}^{FO}\mathfrak{D}_t^\mu \xi(t)$ (see Eq. (2.3)) is approximated using the system $J_O^F Ws$, then for the considered FMPDDEs model in Eq. (1.2), the approximate solution $\xi_{\widehat{m}}(t)$ (see Eq. (4.3)) converges to its exact solution $\xi(t)$.*

Proof. Consider the wavelet approximation of ${}^{FO}\mathfrak{D}_t^\mu \xi(t)$ is ${}^{FO}\mathfrak{D}_t^\mu \xi_{\widehat{m}}(t)$, then we have from Eq. (4.1)

$${}^{FO}\mathfrak{D}_t^\mu \xi(t) \simeq \mathfrak{C}^T \phi \psi^{(\alpha, \beta)}(t) = {}^{FO}\mathfrak{D}_t^\mu \xi_{\widehat{m}}(t).$$

By utilizing Eqs. (4.3) and (5.5), we can express the error as

$$\mathcal{E} = \left\| \xi(t) - \left(\mu \mathfrak{C}^T \phi \mathfrak{M}^{(\alpha, \beta)} \phi \psi^{(\alpha, \beta)}(t) + \xi_0 \right) \right\|.$$

Next, using Eq. (2.6), we get

$$\begin{aligned} \mathcal{E} &= \left\| \left({}^{FO}\mathfrak{J}_t^\mu ({}^{FO}\mathfrak{D}_t^\mu \xi(t)) + \xi_0 \right) - \left(\mu \mathfrak{C}^T \phi \mathfrak{M}^{(\alpha, \beta)} \phi \psi^{(\alpha, \beta)}(t) + \xi_0 \right) \right\| \\ &= \left\| \left({}^{FO}\mathfrak{J}_t^\mu ({}^{FO}\mathfrak{D}_t^\mu \xi(t)) \right) - \left(\mu \mathfrak{C}^T \phi \mathfrak{M}^{(\alpha, \beta)} \phi \psi^{(\alpha, \beta)}(t) \right) \right\|. \end{aligned}$$

According to Eq. (4.2), Lemma 5.3 and Eq. (5.11) w.r.t. Lemma 5.4, we get

$$\begin{aligned} \mathcal{E} &= \left\| {}^{FO}\mathfrak{J}_t^\mu \left({}^{FO}\mathfrak{D}_t^\mu \xi(t) - \mathfrak{C}^T \phi \psi^{(\alpha, \beta)}(t) \right) \right\| \\ &\leq {}^{FO}\mathfrak{J}_t^\mu \left\| \left({}^{FO}\mathfrak{D}_t^\mu \xi(t) - \mathfrak{C}^T \phi \psi^{(\alpha, \beta)}(t) \right) \right\| \\ &\leq {}^{FO}\mathfrak{J}_t^\mu \kappa_1 \|\mathcal{E}_b\| \\ &\leq {}^{FO}\mathfrak{J}_t^\mu \kappa_1 \frac{\mathfrak{L}_\phi}{\Gamma(M\phi + 1)} \frac{1}{\sqrt{(1 + 2M\phi)}}. \end{aligned} \tag{5.12}$$

Now, from Eqs. (5.10) and (5.12), it is evident that as M approaches infinity, \mathcal{E} tends to 0.

Hence, This concludes that the proposed approach is convergent. □

6. METHOD IMPLEMENTATION

Example 6.1. From Eq. (1.2), we have considered the FMPDDE with $p(t) = 0$, $q_1(t) = 1$, $k_1 = 0.5$, and $q_i(t) = k_i = 0 \quad \forall \quad i = 2, 3, \dots, l$ as

$${}^{FO}\mathfrak{D}_t^\mu \xi(t) = \xi(0.5t), \quad 0 < t \leq 1, \tag{6.1}$$

with initial condition,

$$\xi(0) = 1,$$

where ${}^{FO}\mathfrak{D}_t^\mu$ denotes the fractal derivative with fractal order $0 < \mu \leq 1$.

Moreover, if we set $\mu = 1$, Eq. (6.1) simplifies to the classical differential equation, for which the exact solution is given by, see in [33]

$$\xi(t) = \sum_{j=1}^{\infty} \frac{1}{j!} \left(\frac{1}{2} \right)^{\frac{j(j-1)}{2}} t^j.$$

Here, we have solved this example for various $\widehat{m} (= 2^{r-1}M)$ by using the described procedure in section 4 in which an approximate series solution $\xi(t)$ is computed using fractal operators. Subsequently, to obtain the approximate wavelet series solutions, we develop the program code in Mathematica 13.1 to align with the provided pseudo-code. The results for different values of $J_O^F Ws$ (i.e., α , β , and ϕ) and the fractal parameter μ in this example are illustrated in Tables 1 and 2. The exact and approximate solutions for $\mu = \phi = 1$, $\alpha = -\beta = 0.5$, $\widehat{m} = 7$ ($r = 1$, $M = 7$) are shown in



Figure 4(a). Figure 4(b) illustrates an approximate wavelet solution for $\phi = 0.99, \alpha = \beta = 0.5, \widehat{m} = 9$ ($r = 1, M = 9$) and various values of μ . In Figure 5, the estimated error is shown at $\mu = 1, \phi = 1, \alpha = -\beta = 0.5$ with different values of r and M , where the results obtained for $r = 2$ are better than $r = 1$ for the same value of M .

Furthermore, Figure 6 illustrates the contour plots along with their corresponding 3D representations for the Jacobi parameters $-1 < \alpha, \beta < 1$ at the fixed $t = 0.3, 0.5, 0.7, 0.9$.

TABLE 1. Numerical solution obtained at various values of ϕ for Example 6.1.

t	$\mu = 1, \alpha = -\beta = 0.5, r = 1, M = 7$					
	$\phi = 0.3$	$\phi = 0.6$	$\phi = 0.8$	$\phi = 0.9$	$\phi = 0.99$	$\phi = 1.0$
0.1	1.10254	1.10258	1.10224	1.10227	1.10249	1.10252
0.2	1.2102	1.21021	1.21043	1.21028	1.21017	1.21017
0.3	1.32305	1.32297	1.32315	1.32324	1.3231	1.32307
0.4	1.4413	1.44128	1.44109	1.44124	1.44135	1.44135
0.5	1.56512	1.56521	1.56497	1.56494	1.56512	1.56515
0.6	1.69462	1.69472	1.6948	1.69464	1.69458	1.69459
0.7	1.82989	1.82983	1.83015	1.83009	1.82984	1.8298
0.8	1.97102	1.97076	1.97082	1.97097	1.97095	1.97094
0.9	2.11805	2.11799	2.11766	2.11778	2.11808	2.11812
1.0	2.27103	2.27235	2.27359	2.27306	2.2717	2.27149

TABLE 2. Numerical solution obtained at various values of μ for Example 6.1.

t	$\phi = 0.99, \alpha = \beta = 0.5, r = 1, M = 9$					
	$\mu = 0.3$	$\mu = 0.6$	$\mu = 0.8$	$\mu = 0.9$	$\mu = 0.99$	$\mu = 1.0$
0.1	1.67004	1.27528	1.16619	1.13029	1.10499	1.10251
0.3	1.84978	1.43264	1.29851	1.25003	1.21382	1.21017
0.3	1.98846	1.57102	1.42544	1.37009	1.32744	1.32307
0.4	2.10352	1.69905	1.55059	1.49214	1.44612	1.44135
0.5	2.20064	1.81984	1.67535	1.61687	1.57005	1.56515
0.6	2.29018	1.93712	1.80106	1.74491	1.69939	1.69459
0.7	2.37379	2.05193	1.92824	1.87655	1.83428	1.8298
0.8	2.44825	2.16375	2.05687	2.01188	1.97487	1.97094
0.9	2.52076	2.27476	2.18766	2.15123	2.1213	2.11812
1.0	2.58002	2.3821	2.31991	2.29443	2.2737	2.27151

Example 6.2. From Eq. (1.2), we have considered the FMPDDE with $p(t) = 0, q_1(t) = -\frac{5}{4} \exp(-\frac{t}{4}), k_1 = \frac{4}{5}$, and $q_i(t) = k_i = 0, \forall i = 2, 3, \dots, l$ as

$${}^{FO} \mathfrak{D}_t^\mu \xi(t) = -\frac{5}{4} \exp(-0.25t) \xi\left(\frac{4}{5}t\right), \quad 0 < t \leq 1, \tag{6.2}$$

with initial condition,

$$\xi(0) = 1,$$

when we set $\mu = 1$, Eq. (6.2) simplifies to a classical differential equation, and its exact solution is provided as (see [38]):

$$\xi(t) = \exp(-1.25t).$$

Here, we have solved this example for the various values of $\widehat{m} (= 2^{r-1}M)$ by utilizing the described method in section 4 similar to the previous example. The results for different values of $J_O^F Ws$ (i.e. α, β , and ϕ) and the fractal parameter



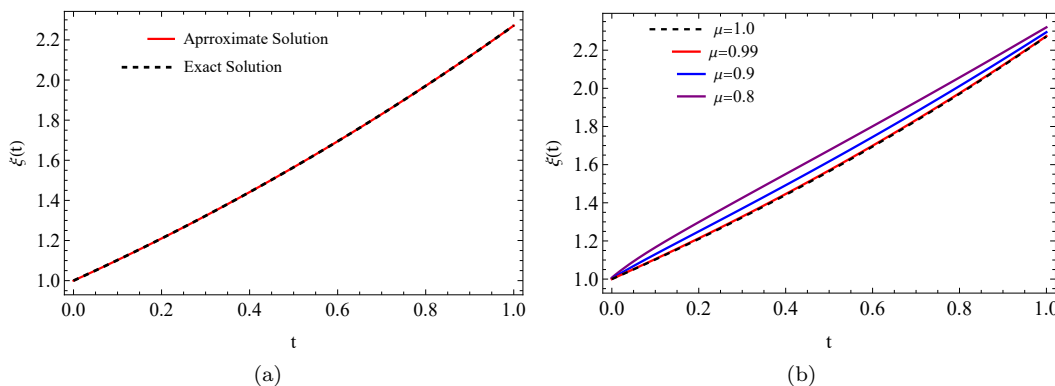


FIGURE 4. Figure 4(a) shows the exact solution and approximate numerical solution for $\mu = \phi = 1, \alpha = -\beta = 0.5, r = 1, M = 7$, and Figure 4(b) shows the approximate numerical solution at $\phi = 0.99, \alpha = \beta = 0.5, r = 1, M = 9$ with different values of μ in Example 6.1.

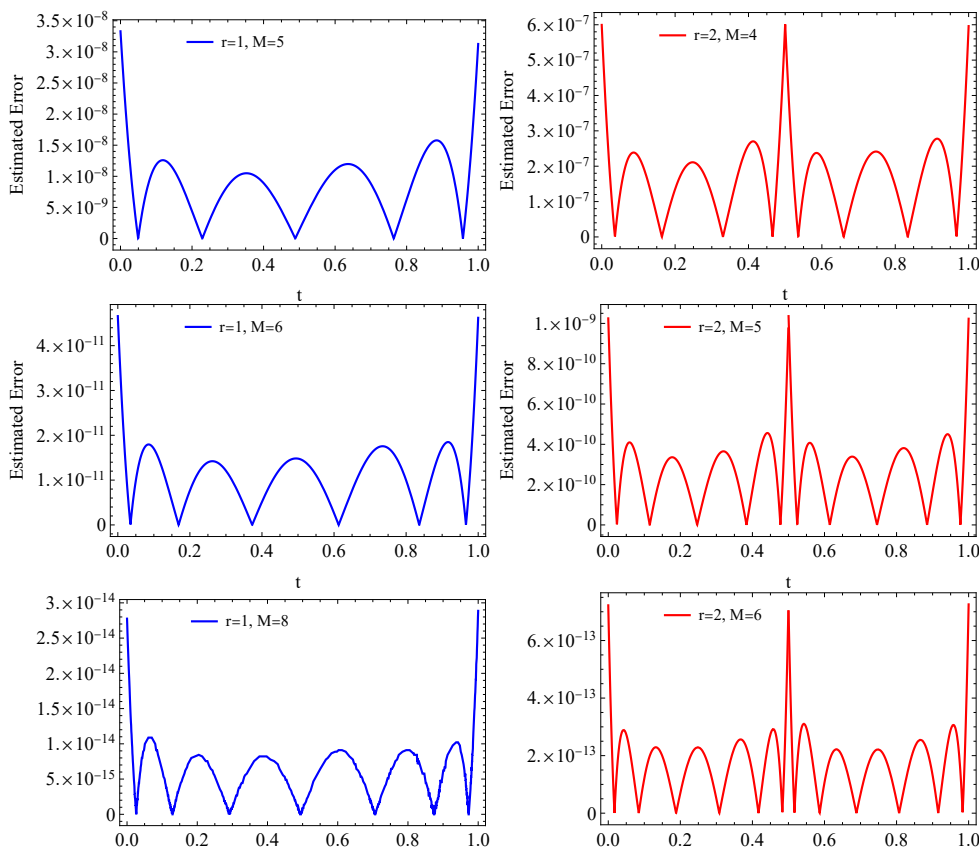


FIGURE 5. Estimated error at $\mu = 1, \phi = 1, \alpha = -\beta = 0.5$ with different value of r and M for Example 6.1.

μ in this example are illustrated in Tables 3 and 4. Also, the absolute error obtained by the proposed method is illustrated in Table 5 with the different values of r and M , where the results obtained for $r = 2$ are better than those for $r = 1$ for the same value of M .



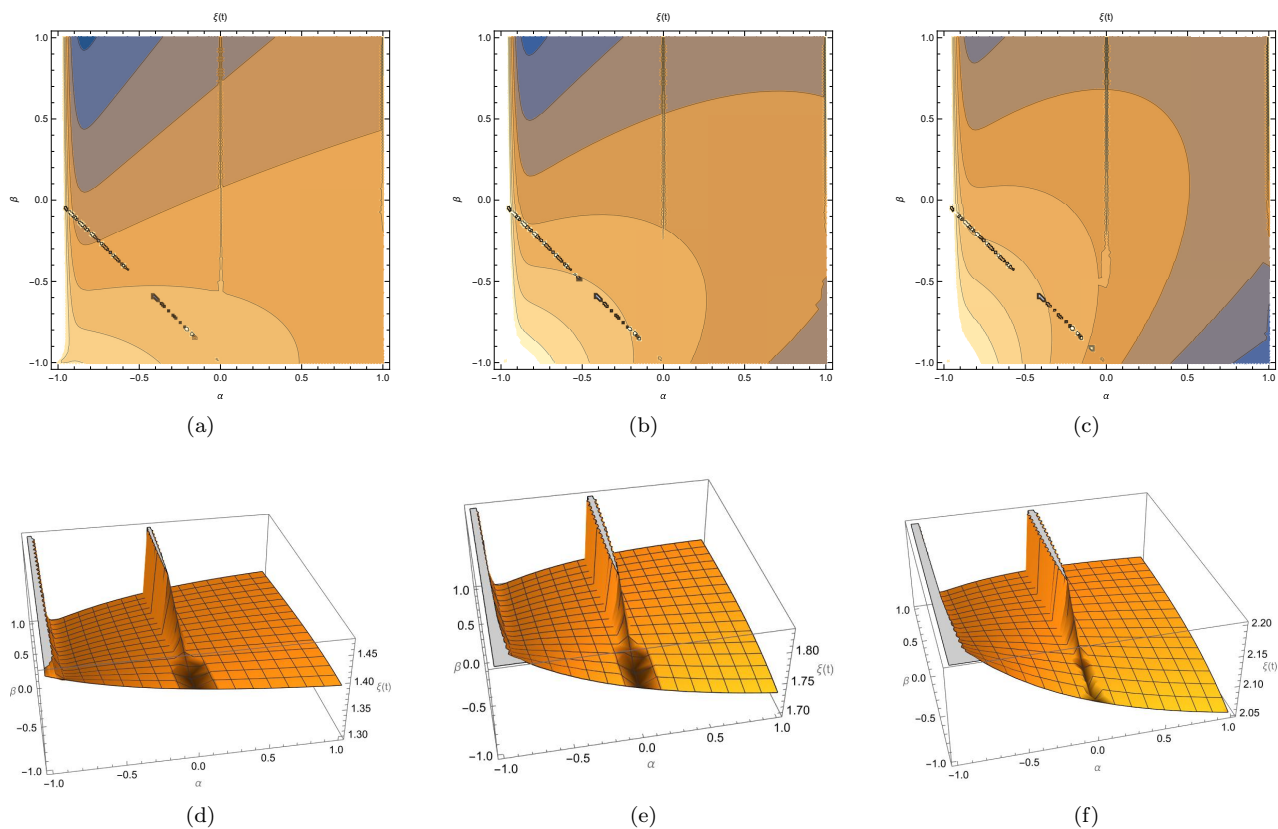


FIGURE 6. Figures 6(a) and 6(d); 6(b) and 6(e); 6(c), and 6(f) depict the contour plots along with their corresponding 3D plots at fixed values of $t = 0.3; 0.6; 0.9$ respectively with $\mu = \phi = 0.9, r = 1, M = 2$ for Example 6.1.

Furthermore, the exact and approximate solutions for $\mu = \phi = 1, \alpha = -\beta = 0.5, \hat{m} = 8 (r = 1, M = 8)$ are shown in Figure 7(a). Figure 7(b) illustrates an approximate wavelet solution for $\phi = 0.99, \alpha = \beta = 0.5, \hat{m} = 9 (r = 1, M = 9)$ and various values of μ . Figure 10 illustrates the contour plots along with their corresponding 3D representations for the Jacobi parameters $-1 < \alpha, \beta < 1$ at the fixed $t = 0.3, 0.5, 0.7, 0.9$. Eq. (5.3) can be used to calculate the errors in the estimation of $\xi(t)$ for different values of ϕ , that is, 0.3, 0.6, 0.9, 1.0. These results are depicted graphically in Figures 8 and 9, showcasing the optimal approximation achieved when $\phi = 1.0$. Also, the error obtained by the present scheme is $\simeq 10^{-9}$ while by the given scheme in [38] is $\simeq 10^{-8}$ for $\mu = 1$, which shows that the present scheme gives a more accurate solution.

Example 6.3. From Eq. (1.2), we have considered the FMPDDE with $p(t) = -1, F(t) = -\frac{1}{10} \exp(-\frac{t}{5}), q_1(t) = \frac{1}{10}, k_1 = \frac{1}{5},$ and $q_i(t) = k_i = 0, \forall i = 2, 3, \dots, l$ as

$${}^{FO} \mathcal{D}_t^\mu \xi(t) = -\xi(t) + \frac{1}{10} \xi\left(\frac{t}{5}\right) - \frac{1}{10} \exp\left(-\frac{t}{5}\right), \quad 0 < t \leq 1, 0 < \mu \leq 1, \tag{6.3}$$

with initial condition,

$$\xi(0) = 1.$$



TABLE 3. Numerical solution obtained at various values of ϕ for Example 6.2.

t	$\mu = 1, \alpha = \beta = 0, r = 1, M = 8$					
	$\phi = 0.3$	$\phi = 0.6$	$\phi = 0.8$	$\phi = 0.9$	$\phi = 0.99$	$\phi = 1.0$
0.1	0.882527	0.882456	0.882657	0.882664	0.882515	0.882497
0.2	0.778822	0.778808	0.778666	0.778731	0.778801	0.778801
0.3	0.68732	0.687327	0.687316	0.687242	0.687277	0.687289
0.4	0.606561	0.606522	0.606643	0.606615	0.606538	0.606531
0.5	0.535278	0.535225	0.535245	0.5353	0.535271	0.535261
0.6	0.472372	0.472361	0.47227	0.4723	0.472361	0.472367
0.7	0.416869	0.416897	0.416874	0.416836	0.416855	0.416862
0.8	0.367901	0.367897	0.367976	0.367953	0.367888	0.367879
0.9	0.324678	0.324614	0.324585	0.32462	0.32465	0.324652
1.0	0.286482	0.286599	0.286766	0.286699	0.286528	0.286505

TABLE 4. Numerical solution obtained at various values of μ for Example 6.2.

t	$\phi = 0.99, \alpha = -\beta = 0.5, r = 1, M = 9$					
	$\mu = 0.3$	$\mu = 0.6$	$\mu = 0.8$	$\mu = 0.9$	$\mu = 0.99$	$\mu = 1.0$
0.1	0.524252	0.725027	0.818662	0.853802	0.879904	0.882516
0.2	0.472669	0.621202	0.707569	0.745114	0.775587	0.778781
0.3	0.408614	0.538864	0.618182	0.654032	0.684093	0.687305
0.4	0.384056	0.482154	0.546602	0.577193	0.603662	0.606538
0.5	0.373837	0.439497	0.487332	0.511392	0.532873	0.535244
0.6	0.342762	0.397436	0.43518	0.453845	0.470523	0.472369
0.7	0.319789	0.362554	0.390435	0.403771	0.415577	0.41688
0.8	0.326975	0.340704	0.353638	0.360643	0.367133	0.367862
0.9	0.297202	0.31142	0.318981	0.321982	0.324408	0.324665
1.0	0.385343	0.318994	0.296726	0.290617	0.286716	0.286347

TABLE 5. Absolute error for various values of r and M with $\phi = 1.0, \alpha = \beta = 0$ for Example 6.2.

t	Absolute error obtained for $r = 1$			Absolute error obtained for $r = 2$		
	$M = 5$	$M = 6$	$M = 8$	$M = 4$	$M = 5$	$M = 6$
0.2	8.9×10^{-6}	4.605×10^{-7}	7.899×10^{-10}	16.30×10^{-6}	6.677×10^{-7}	7.859×10^{-9}
0.4	15.2×10^{-6}	4.552×10^{-7}	6.380×10^{-10}	28.87×10^{-6}	3.021×10^{-7}	1.081×10^{-8}
0.6	19.9×10^{-6}	3.518×10^{-7}	5.126×10^{-10}	17.19×10^{-6}	2.676×10^{-7}	4.202×10^{-9}
0.8	6.71×10^{-6}	5.345×10^{-7}	9.038×10^{-10}	8.306×10^{-6}	4.534×10^{-7}	6.839×10^{-9}
1.0	2.06×10^{-5}	1.143×10^{-6}	5.315×10^{-9}	2.389×10^{-5}	9.386×10^{-8}	2.365×10^{-9}

Moreover, when we set $\mu = 1$, Eq. (6.3) simplifies to a classical differential equation, and its exact solution is provided as (see in [15]):

$$\xi(t) = \exp(-t).$$

We solved this example for various values of $\hat{m} (= 2^{r-1}M)$ by utilizing the described method in a similar way to the previous examples. The results for different values of $J_O^F Ws$ (i.e. $\alpha, \beta,$ and ϕ) and the fractal parameter μ in this example are illustrated in Tables 6 and 7. Also, the absolute error obtained by the proposed method and the presented method in [15] are illustrated in Table 8, in which the comparison has been shown for the same number of basis functions $M = N + 1$, which shows that the proposed method gives a more accurate solution.



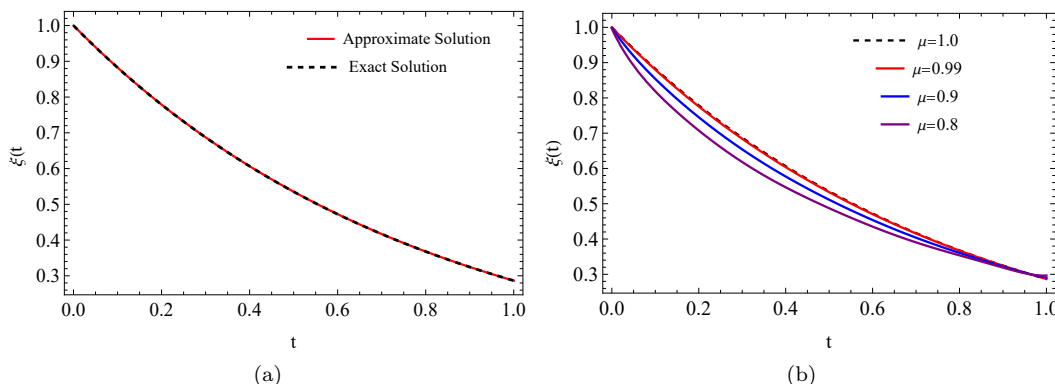


FIGURE 7. Figure 7(a) shows the exact solution and approximate numerical solution for $\mu = \phi = 1, \alpha = \beta = 0, r = 2, M = 5$, and Figure 7(b) shows the approximate numerical solution at $\phi = 0.99, \alpha = -\beta = 0.5, r = 1, M = 9$ with different values of μ in Example 6.2.

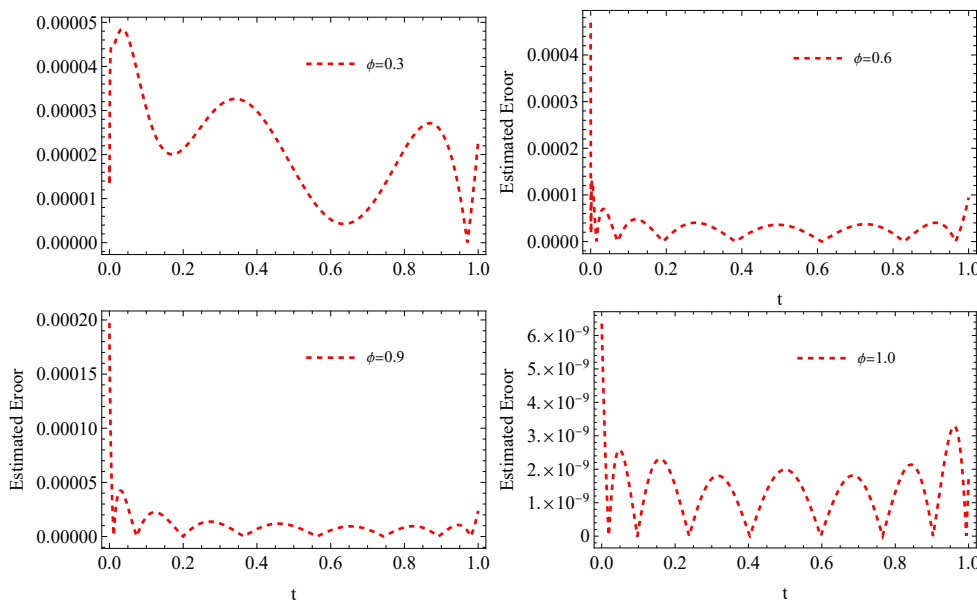


FIGURE 8. Estimated error at $\mu = 1, \alpha = \beta = 0, r = 1, M = 8$ with different value of ϕ for Example 6.2.

The exact and approximate solutions for $\mu = \phi = 1, \alpha = \beta = 0, \hat{m} = 9 (r = 1, M = 9)$ are depicted in Figure 11(a). Figure 11(b) illustrates an approximate wavelet solutions for $\phi = 0.99, \alpha = -\beta = 0.5, \hat{m} = 11 (r = 1, M = 11)$, and various values of μ . Eq. (5.3) can be used to calculate the errors in the estimation of $\xi(t)$ for different values of ϕ . These results are depicted graphically in Figures 12 and 13, showcasing the optimal approximation achieved when $\phi = 1.0$.

7. CONCLUSION

In this research, the fractal derivative was used to introduce a new model of the MPDDEs with varying coefficients defined as FMPDDEs. This model offers a comprehensive representation of fractal PDDEs, with practical applications spanning various fields. We introduced $J_O^F Ws$ in this study, which generalize various wavelets (such as Legendre, Chebyshev 1st and 2nd kind, Gegenbauer, etc.) for fractional orders. Subsequently, this study introduces an approximate procedure that integrates the FIOM of the $J_O^F Ws$ with a collocation technique to handle FMPDDEs



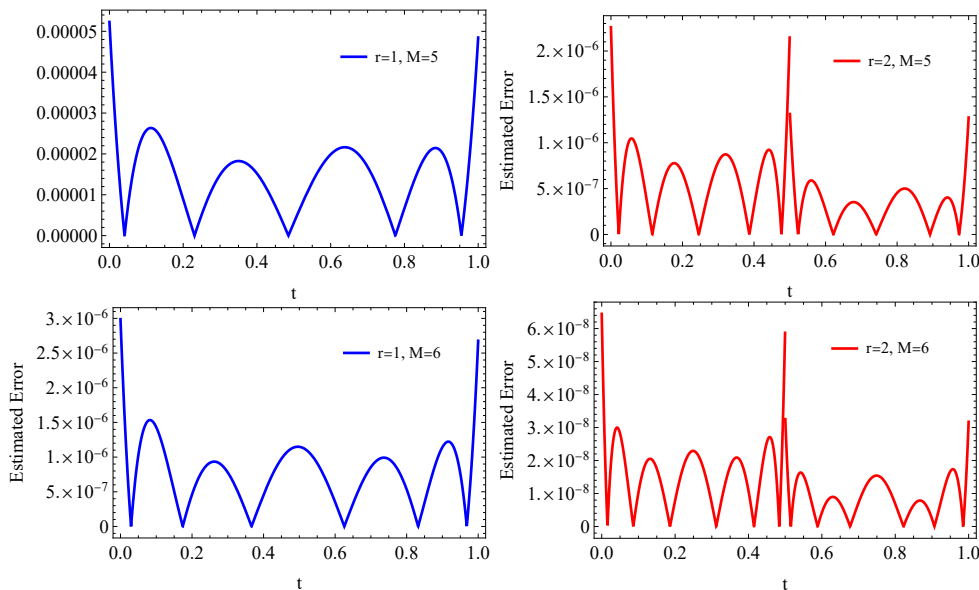


FIGURE 9. Estimated error at $\mu = 1, \phi = 1, \alpha = \beta = 0$ with different value of r and M for Example 6.2.

TABLE 6. Numerical solution obtained at various values of ϕ for Example 6.3.

t	$\mu = 1, \alpha = \beta = 0, r = 1, M = 11$					
	$\phi = 0.3$	$\phi = 0.6$	$\phi = 0.8$	$\phi = 0.9$	$\phi = 0.99$	$\phi = 1.0$
0.1	0.904837	0.904845	0.904794	0.904817	0.904839	0.904837
0.2	0.818731	0.818724	0.818762	0.818747	0.81873	0.818731
0.3	0.740818	0.74082	0.740796	0.740816	0.74082	0.740818
0.4	0.67032	0.670324	0.670325	0.670307	0.670317	0.67032
0.5	0.606531	0.606525	0.606547	0.606549	0.606532	0.606531
0.6	0.548812	0.548811	0.548792	0.548804	0.548812	0.548812
0.7	0.496585	0.496591	0.49659	0.496578	0.496583	0.496585
0.8	0.449329	0.449325	0.44934	0.449344	0.449331	0.449329
0.9	0.40657	0.40657	0.406552	0.406551	0.406567	0.40657
1.0	0.367879	0.367859	0.367809	0.367822	0.367872	0.367879

characterized by variable coefficients associated with FD. This approach is used to analyze some problems. The main advantage of this proposed approach is its ability to achieve highly accurate and satisfactory results using fewer wavelet bases. The solutions to FMPDDEs with variable coefficients are presented both in tabular format and graphically. It is evident from the tables and Figures that the behavior of the FO is smoother and yields classical solutions as $\mu \rightarrow 1$. Also, the numerical results can be improved by increasing the values of r and M . It is worth noting how straightforward and simple the proposed approach is to implement.

8. SIGNIFICANCE

The significance of the FMPDDEs lies in their ability to model complex, memory-dependent systems with fractal behavior, making it a valuable tool for understanding and predicting the behavior of diverse real-world phenomena, such as electrocardiogram analysis in biological signaling, fractional Brownian motion in engineering particle tracking models, Brownian motion in physics, stock price predictions using geometric Brownian motion, stochastic processes, etc.



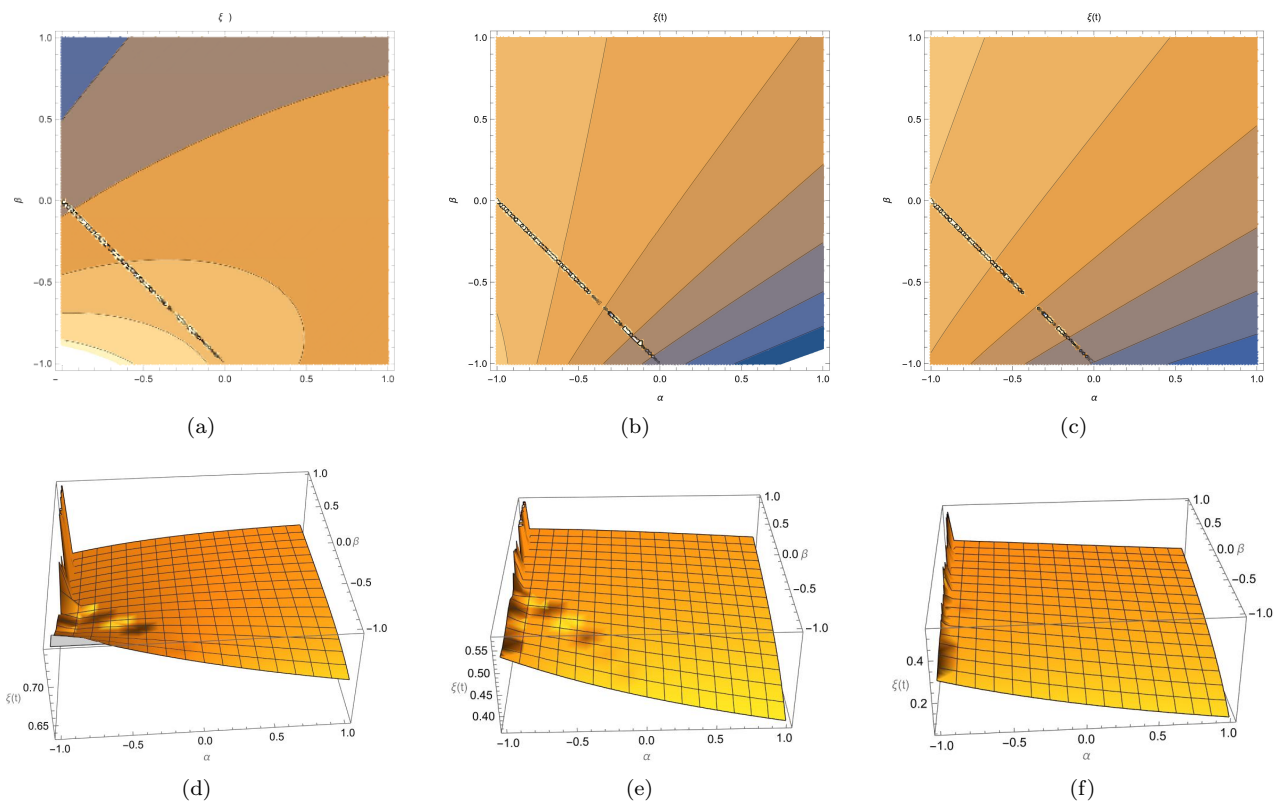


FIGURE 10. Figures 10(a) and 10(d); 10(b) and 10(e); 10(c) and 10(f) depict the contour plots along with their corresponding 3D plots at fixed values of $t = 0.3; 0.6; 0.9$ respectively with $\mu = 0.9$, $\phi = 1, r = 1, M = 2$ for Example 6.2.

TABLE 7. Numerical solution obtained at various values of μ for Example 6.3.

t	$\phi = 0.99, \alpha = -\beta = 0.5, r = 1, M = 11$					
	$\mu = 0.3$	$\mu = 0.6$	$\mu = 0.8$	$\mu = 0.9$	$\mu = 0.99$	$\mu = 1.0$
0.1	0.60866	0.778333	0.853522	0.88173	0.902728	0.904832
0.2	0.528512	0.680375	0.758115	0.790375	0.816064	0.818736
0.3	0.491537	0.612852	0.681926	0.712606	0.738105	0.740818
0.4	0.462304	0.558962	0.617541	0.644662	0.667816	0.670315
0.5	0.427523	0.511263	0.561216	0.5844	0.604369	0.606538
0.6	0.416807	0.475102	0.512876	0.531081	0.547056	0.548807
0.7	0.396436	0.440909	0.469454	0.483184	0.495258	0.496584
0.8	0.37477	0.409723	0.430474	0.440086	0.448425	0.449336
0.9	0.373729	0.386503	0.396544	0.401588	0.406067	0.40656
1.0	0.422224	0.377948	0.368754	0.367691	0.367749	0.367793

Moreover, $J^E Ws$ provide a robust and versatile method for numerically approximating solutions to DDEs. Their attributes such as orthogonality, adaptability, multi-resolution analysis, sparse representation, numerical stability, and wide applicability render them indispensable for addressing the complexities inherent in modeling and simulating delayed systems across various scientific and engineering domains. By adjusting parameters like α and β in the



TABLE 8. Absolute error for various values of M with $\phi = 1.0, \alpha = \beta = 0, r = 1$ for Example 6.3.

t	Absolute error obtained by the proposed method			Absolute error obtained by the method in [15]	
	$M = 7$	$M = 9$	$M = 11$	$N = 6 (M = 7)$	$N = 10 (M = 11)$
2^{-1}	4.62×10^{-10}	5.84×10^{-13}	2.22×10^{-16}	2.12×10^{-8}	2.52×10^{-14}
2^{-2}	7.47×10^{-9}	9.44×10^{-12}	1.44×10^{-15}	2.26×10^{-8}	3.04×10^{-14}
2^{-3}	4.75×10^{-10}	1.09×10^{-11}	1.99×10^{-15}	2.92×10^{-8}	3.84×10^{-14}
2^{-4}	1.44×10^{-8}	8.09×10^{-12}	2.22×10^{-15}	1.48×10^{-8}	3.53×10^{-14}
2^{-5}	4.86×10^{-9}	1.26×10^{-11}	8.44×10^{-15}	5.12×10^{-9}	1.69×10^{-14}
2^{-6}	1.01×10^{-8}	2.19×10^{-13}	4.77×10^{-15}	1.49×10^{-9}	5.81×10^{-15}

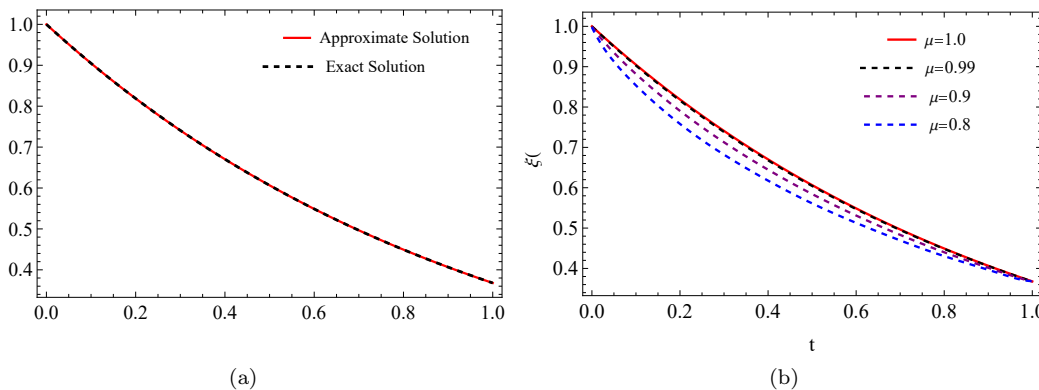


FIGURE 11. Figure 11(a) shows the exact solution and approximate numerical solution for $\mu = \phi = 1, \alpha = \beta = 0, r = 2, M = 9$ and Figure 11(b) shows the approximate numerical solution at $\phi = 0.99, \alpha = -\beta = 0.5, r = 1, M = 11$ with different values of μ in Example 6.3.

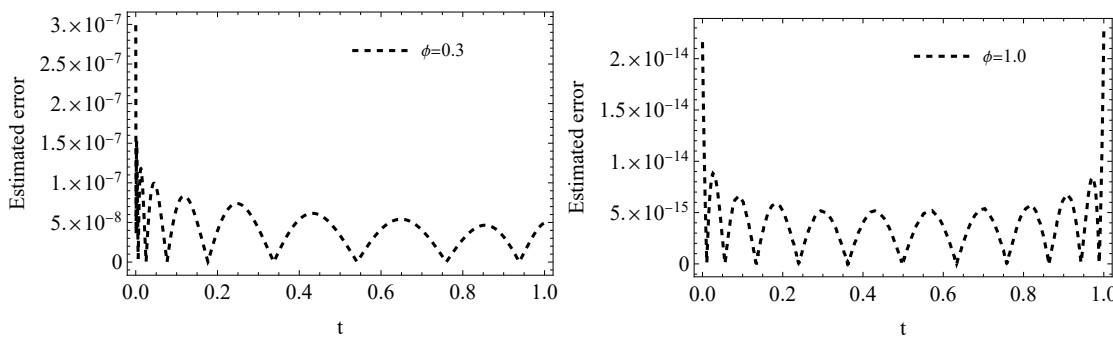


FIGURE 12. Estimated error at $\mu = 1, \alpha = \beta = 0, r = 1, M = 11$ with different values of ϕ in Example 6.3.

Jacobi fractional polynomials, these $J_O^F W$ s can be customized to match specific characteristics of the delay function, encompassing features such as smoothness, decay rates, and oscillatory behavior, which can be easily seen in Figures 6 and 10 for the considered examples. This adaptability ensures the $J_O^F W$ s basis can effectively capture the dynamic behavior of the delayed system, enhancing the accuracy and reliability of the numerical solutions.



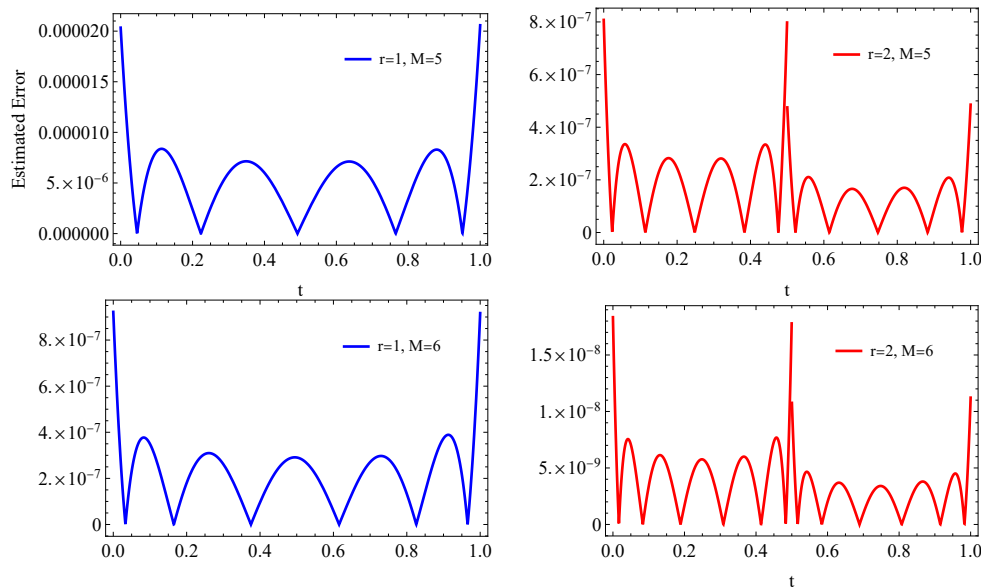


FIGURE 13. Estimated error at $\mu = 1$, $\phi = 1$, $\alpha = \beta = 0$ with different value of r and M for Example 6.3.

COMPLIANCE WITH ETHICAL STANDARDS

The authors confirm no conflicts of interest related to this study. This research is entirely unique and has not appeared in any other format or language. It is being submitted to this journal for the first time and has not been simultaneously submitted elsewhere. The results presented in this manuscript are transparent, truthful, and have not been subject to any form of falsification or improper data manipulation.

ACKNOWLEDGMENT

First author would like to thank the University Grant Commission (UGC), New Delhi, India, for providing financial support as a junior research fellow (JRF) through NTA Ref. No.: 191620168793. It's important to note that no funding support was received for its publication. The authors are very grateful to the reviewer for carefully reading the manuscript and for giving such valuable suggestions and comments which have improved the quality and presentation of this manuscript.

REFERENCES

- [1] A. Allwright and A. Atangana, *Fractal advection-dispersion equation for groundwater transport in fractured aquifers with self-similarities*, The European Physical Journal Plus, *133* (2018), 1-20.
- [2] A. A. Arbuzov and R. R. Nigmatullin, *Three-dimensional fractal models of electrochemical processes*, Russian Journal of Electrochemistry, *45* (2009), 1276-1286.
- [3] A. Atangana and S. Jain, *A new numerical approximation of the fractal ordinary differential equation*, The European Physical Journal Plus, *133* (2018), 1-15.
- [4] M. M. Bahşi and M. Çevik, *Numerical solution of pantograph-type delay differential equations using perturbation-iteration algorithms*, Journal of Applied Mathematics, *2015*(1) (2015), 139821.
- [5] C. T. Baker, C. A. Paul, and D. R. Willé, *Issues in the numerical solution of evolutionary delay differential equations*, Advances in Computational Mathematics, *3* (1995), 171-196.
- [6] C. C. Barton, P. A. Hsieh, J. Angelier, F. Bergerat, C. Bouroz, and M. Dettinger, *Physical and Hydrologic-flow Properties of Fractures: Las Vegas, Nevada-Zion Canyon, Utah-Grand Canyon, Arizona-Yucca Mountain, Nevada, July 20-24, 1989*, Washington, DC: American Geophysical Union, (1989).



- [7] M. Basim, A. Ahmadian, N. Senu, and Z. B. Ibrahim, *Numerical simulation of variable-order fractal-fractional delay differential equations with nonsingular derivative*, Engineering Science and Technology, an International Journal, *42* (2023), 101412.
- [8] A. H. Bhrawy and M. A. Zaky, *Shifted fractional-order Jacobi orthogonal functions: application to a system of fractional differential equations*, Appl. Math. Model, *40*(2) (2016), 832-845.
- [9] W. Chen, H. Sun, X. Zhang, and D. Korošak, *Anomalous diffusion modeling by fractal and fractional derivatives*, Computers & Mathematics with Applications, *59*(5) (2010), 1754-1758.
- [10] Y. Chen, *Fractal Modeling and fractal dimension description of urban morphology*, Entropy, *22*(9) (2020), 961.
- [11] G. Chi, and G. Li, *Numerical identification of the fractal orders in the generalized nonlocal elastic model*, Journal of Engineering Mathematics *142*(1) (2023), 4.
- [12] C. K. Chui, *Wavelets: a mathematical tool for signal analysis*, Society for Industrial and Applied Mathematics, 1997.
- [13] W. Dahmen *Wavelet and multiscale methods for operator equations*, Acta numerica, *6* (1997), 55-228.
- [14] I. Daubechies, *Ten lectures on wavelets*, Society for industrial and applied mathematics, 1992.
- [15] H. Dehestani, Y. Ordokhani, and M. Razzaghi, *Fractional-order Bessel functions with various applications*, Applications of Mathematics, *64* (2019), 637-662.
- [16] A. El-Ajou, N. O. Moa'ath, Z. Al-Zhour, and S. Momani, *Analytical numerical solutions of the fractional multi-pantograph system: Two attractive methods and comparisons*, Results in Physics, *14* (2019), 102500.
- [17] N. A. Elkot, E. H. Doha, I. G. Ameen, A. S. Hendy, and M. A. Zaky, *A re-scaling spectral collocation method for the nonlinear fractional pantograph delay differential equations with non-smooth solutions*, Communications in Nonlinear Science and Numerical Simulation, *118* (2023), 107017.
- [18] J. Haškovec, *Asymptotic and exponential decay in mean square for delay geometric Brownian motion*, Applications of Mathematics, (2022), 1-13.
- [19] J. H. He, *A new fractal derivation*, Thermal science, *15*(suppl.1) (2011), 145-147.
- [20] O. R. Isik, and T. Turkoglu, *A rational approximate solution for generalized pantograph-delay differential equations*, Mathematical Methods in the Applied Sciences, *39*(8) (2016), 2011-2024.
- [21] M. T. Kajani, *Numerical solution of fractional pantograph equations via Müntz–Legendre polynomials*, Mathematical Sciences, *18*(3) (2024), 387-395.
- [22] A. Karoui, *Wavelets: Properties and approximate solution of a second kind integral equation*, Computers & Mathematics with Applications, *46*(2-3) (2003), 263-277.
- [23] M. A. Khan, and A. Atangana, *Numerical methods for fractal-fractional differential equations and engineering: simulations and modeling*, CRC Press, (2023).
- [24] C. King, *Fractal geography of the Riemann zeta function*, arXiv preprint arXiv:1103.5274, (2011).
- [25] M. Li, M. Fečkan, and J. Wang, *Finite time stability and relative controllability of second order linear differential systems with pure delay*, Applications of Mathematics, *68*(3) (2023), 305-327.
- [26] Y. Li, and Y. Shao, *Dynamic analysis of an impulsive differential equation with time-varying delays*, Applications of Mathematics, *59*(1) (2014), 85-98.
- [27] D. Lu, Y. Chen, R. Mehdi, S. Jabeen, and A. Rashid, *Approximate solution of multi-pantograph equations with variable coefficients via collocation method based on hermite polynomials*, Communications in Mathematics and Applications, *9*(4) (2018), 601.
- [28] J. R. Ockendon, and A. B. Tayler, *The dynamics of a current collection system for an electric locomotive*, Proceedings of the Royal Society of London. A. Mathematical and Physical Sciences, *322*(1551) (1971), 447-468.
- [29] N. Pashmakian, A. Farajzadeh, N. Parandin, and N. Karamikabir, *A numerical approach for solving the Fractal ordinary differential equations*, Computational Methods for Differential Equations, *12*(4) (2024), 780-790.
- [30] Y. Rahrovi, Y. Mahmoudi, A. S. Shamloo, and M. J. Rad, *Jacobi wavelets method for numerical solution of fractional population growth model*, Computational Methods for Differential Equations, *11*(2) (2023), 387-398.
- [31] S. A. Rakhshan, and S. Effati, *A generalized Legendre–Gauss collocation method for solving nonlinear fractional differential equations with time varying delays*, Applied Numerical Mathematics, *146* (2019), 342-360.



- [32] A. Rayal, and S. R. Verma, *An approximate wavelets solution to the class of variational problems with fractional order*, Journal of Applied Mathematics and Computing, 651 (2021), 735-769.
- [33] A. Rayal, and S. R. Verma, *Numerical analysis of pantograph differential equation of the stretched type associated with fractal-fractional derivatives via fractional order Legendre wavelets*, Chaos, Solitons & Fractals, 139 (2020), 110076.
- [34] J. A. Rodrigues, and V. C. Pandolfelli, *Insights on the fractal-fracture behaviour relationship*, Materials Research, 1 (1998), 47-52.
- [35] A. Roy, E. Perfect, W. M. Dunne, and L. D. McKay, *Fractal characterization of fracture networks: An improved box-counting technique*, Journal of Geophysical Research: Solid Earth, 112(B12) (2007).
- [36] S. Sabermahani, Y. Ordokhani, and M. Razzaghi, *Ritz-generalized Pell wavelet method: Application for two classes of fractional pantograph problems*, Communications in Nonlinear Science and Numerical Simulation, 119 (2023), 107138.
- [37] S. Sabermahani, Y. Ordokhani, and P. Rahimkhani, *Application of generalized Lucas wavelet method for solving nonlinear fractal-fractional optimal control problems*, Chaos, Solitons & Fractals, 170 (2023), 113348.
- [38] S. Sedaghat, Y. Ordokhani, and M. Dehghan, *Numerical solution of the delay differential equations of pantograph type via Chebyshev polynomials*, Communications in Nonlinear Science and Numerical Simulation, 17(12) (2012), 4815-4830.
- [39] M. Sezer, and N. Şahin, *Approximate solution of multi-pantograph equation with variable coefficients*, Journal of Computational and Applied Mathematics, 214(2) (2008), 406-416.
- [40] T. Shojaeizadeh, M. Mahmoudi, and M. Darehmira, *Optimal control problem of advection-diffusion-reaction equation of kind fractal-fractional applying shifted Jacobi polynomials*, Chaos, Solitons & Fractals, 143 (2021), 110568.
- [41] A. B. Tayler, *Mathematical models in applied mechanics*, Oxford University Press, 4 (2001).
- [42] K. L. Wang, *A novel computational approach to the local fractional Lonngren wave equation in fractal media*, Mathematical Sciences, 18(3) (2024), 413-418.
- [43] X. J. Yang, D. Baleanu, and H. M. Srivastava, *Local fractional integral transforms and their applications*, Academic Press, (2015).
- [44] F. Zhao, J. Hu, T. Liu, T. Zhou, and Q. Ren, *Study of the macro and micro characteristics of and their relationships in cemented backfill based on SEM*, Materials, 16(13) (2023), 4772.
- [45] H. Zhou, F. Duan, Z. Liu, L. Chen, Y. Song, and Y. Zhang, *Study on electric spark discharge between pantograph and catenary in electrified railway*, IET Electrical Systems in Transportation, 12(2) (2022), 128-142.

